

## Classification of four-Reggeon states in multi-colour QCD

**Jan Koteński**

M. Smoluchowski Institute of Physics, Jagellonian University  
Reymonta 4, 30-059 Kraków, Poland

$N$ -Reggeized gluon states in Quantum Chromodynamics are described by BKP equation. In order to solve this equation for  $N > 3$  particles the  $Q$ -Baxter operator method is used. Spectrum of the integrals of motion of the system exhibits a complicated structure. In this work we consider the case with  $N = 4$  Reggeons where complicated relations between  $q_3$ -spectrum and  $q_4$ -spectrum are analysed. Moreover, corrections to WKB approximation for  $N = 4$  and  $q_3 = 0$  are computed.

PACS numbers: 12.40.Nn, 11.55.Jy, 12.38.-t, 12.38.-t

*Keywords:* Reggeons, QCD, spectrum, eigenstates

TPJU-04/2006

## 1. Introduction

In the Regge limit, where the total energy  $s$  is large while the transfer of four-momentum  $t$  is low and fixed, the scattering amplitude of two hadrons can be rewritten as an exchange of effective particles, *i.e.* propagating in  $t$ -channel reggeized gluons, which are also called Reggeons [1, 2, 3, 4, 5, 6].

Due to ordering of generalized leading logarithm approximation contribution from exchange of  $N$ -Reggeon states is suppressed by factor  $\alpha_s^{N-2}$  where  $\alpha_s$  is a strong coupling constant. Thus, the leading contribution is given by two Reggeon states, *i.e.* BFKL Pomeron. The equation describing this case was firstly derived and solved by Balitsky, Fadin, Kuraev and Lipatov [7, 8, 4]. Extension of this equation for more than two Reggeons was formulated in 1980 [9, 10, 11] by Bartels, Kwieciński, Praszalowicz and Jaroszewicz. It has a structure of Schrödinger equation. The first solutions for exchange of three Reggeons appear in nineties [12, 13, 14] and these solutions correspond to leading contribution to the QCD odderon state as well as subleading contribution to the Pomeron state.

The Schrödinger equation for  $N \geq 4$  Reggeons contains complicated colour factor and even in 't Hooft's multi-colour limit [23, 24, 25], *i.e.*  $N_c \rightarrow \infty$ , formulating of its solutions poses real challenge and demands using of advanced methods of integrable systems. In the multi-colour limit the Reggeon Hamiltonian corresponds to the Hamiltonian  $SL(2, \mathbb{C})$  spin magnet which turns out to be solvable model. Thus, making use of  $Q$ -Baxter and Separation of Variable methods one can solve the multi-Reggeon problem in multi-colour limit. The solutions for higher  $N = 4, \dots, 8$  were obtained recently in series of papers [15, 16, 17] written in collaboration with S.É. Derkachov, G.P. Korchemsky and A.N. Manashov. Similar results for  $N = 4$  appear also in Ref. [18, 19].

The present work is continuation of [20] as well as [15, 16, 17]. We concentrate on  $N = 4$  case with conformal Lorentz spin  $n_h = 0$ . Here, classification of the four Reggeon states is performed and corrections to the WKB calculation are computed. Moreover, we calculate the rich spectrum of the the Reggeon energy and the conformal charges  $\{q_3, q_4\}$  for four reggeized gluons. For a broader perspective see also Ref. [21].

Thus, in Section 2 we explain when the reggeization of the gluon appears [22]. Next, we perform the multi-colour limit [23, 24, 25], discuss the properties of the  $SL(2, \mathbb{C})$  symmetry and construct invariants of this symmetry, the conformal charges. In Section 3 we introduce a Baxter  $Q$ -operator method [26] with Baxter equations that allow us to solve the Reggeon system, completely. Next, we present the exact solution to the Baxter equations. It consists in rewriting the Baxter equation into the differential equation, which may be solved by a series method. We find the quantization conditions for

$\{q_3, q_4\}$  which come analyticity properties of the Baxter functions. We also recapitulate known properties of  $N$ -Reggeon spectrum. The numerical results are shown in Section 6 [16, 17]. In particular, we discuss the resemblant and winding structures of the  $q_4$  and  $q_3$  spectrum and also corrections to the WKB approximation for  $q_3 = 0$ . At the end we make final conclusions.

## 2. System with $SL(2, \mathbb{C})$ symmetry

### 2.1. Hamiltonian

In the Regge limit

$$s \rightarrow \infty \text{ and } t = \text{const} \quad (2.1)$$

$N$ -Reggeon Hamiltonian can be rewritten as a sum of BFKL kernels. Performing the multi-colour limit [23, 24, 25], where a number of colours  $N_c \rightarrow \infty$ , the system of  $N$ -reggeized gluons is described by Hamiltonian

$$\mathcal{H}_N = H_N + \bar{H}_N, \quad [H_N, \bar{H}_N] = 0 \quad (2.2)$$

which can be written in terms of the conformal spins (2.7):

$$H_N = \sum_{k=1}^N H(J_{k,k+1}), \quad \bar{H}_N = \sum_{k=1}^N H(\bar{J}_{k,k+1}), \quad (2.3)$$

where

$$H(J) = \psi(1 - J) + \psi(J) - 2\psi(1) \quad (2.4)$$

with  $\psi(x) = d \ln \Gamma(x) / dx$  being the Euler function and  $J_{N,N+1} = J_{N,1}$ . Here operators,  $J_{k,k+1}$  and  $\bar{J}_{k,k+1}$ , are defined through the Casimir operators for the sum of the spins of the neighbouring Reggeons

$$J_{k,k+1}(J_{k,k+1} - 1) = (S^{(k)} + S^{(k+1)})^2 \quad (2.5)$$

with  $S_\alpha^{(N+1)} = S_\alpha^{(1)}$ , and  $\bar{J}_{k,k+1}$  is defined similarly.

### 2.2. Symmetry $SL(2, \mathbb{C})$

The Hamiltonian (2.2) is invariant under the coordinate transformation of the  $SL(2, \mathbb{C})$  group

$$z'_k = \frac{az_k + b}{cz_k + d}, \quad \bar{z}'_k = \frac{\bar{a}\bar{z}_k + \bar{b}}{\bar{c}\bar{z}_k + \bar{d}} \quad (2.6)$$

with  $k = 1, \dots, N$  and  $ad - bc = \bar{a}\bar{d} - \bar{b}\bar{c} = 1$ .

Now, one may associate with the  $k$ -th particle the generators of this transformation [27]. These generators are a pair of mutually commuting holomorphic and anti-holomorphic spin operators,  $S_\alpha^{(k)}$  and  $\bar{S}_\alpha^{(k)}$ . They satisfy the standard commutation relations  $[S_\alpha^{(k)}, S_\beta^{(n)}] = i\epsilon_{\alpha\beta\gamma}\delta^{kn}S_\gamma^{(k)}$  and similarly for  $\bar{S}_\alpha^{(k)}$ . The generators act on the quantum space of the  $k$ -th particle,  $V^{(s_k, \bar{s}_k)}$  as differential operators

$$\begin{aligned} S_0^k &= z_k \partial_{z_k} + s_k, & S_-^{(k)} &= -\partial_{z_k}, & S_+^{(k)} &= z_k^2 \partial_{z_k} + 2s_k z_k, \\ \bar{S}_0^k &= \bar{z}_k \partial_{\bar{z}_k} + \bar{s}_k, & \bar{S}_-^{(k)} &= -\partial_{\bar{z}_k}, & \bar{S}_+^{(k)} &= \bar{z}_k^2 \partial_{\bar{z}_k} + 2\bar{s}_k \bar{z}_k, \end{aligned} \quad (2.7)$$

where  $S_\pm^{(k)} = S_1^{(k)} \pm iS_2^{(k)}$  while the complex parameters,  $s_k$  and  $\bar{s}_k$ , are called the complex spins. Thus, the Casimir operator reads

$$\sum_{j=0}^2 (S_j^{(k)})^2 = (S_0^{(k)})^2 + (S_+^{(k)} S_-^{(k)} + S_-^{(k)} S_+^{(k)})/2 = s_k(s_k - 1) \quad (2.8)$$

and similarly for the anti-holomorphic operator  $(\bar{S}^{(k)})^2$ .

The eigenstates of  $\text{SL}(2, \mathbb{C})$  invariant system transform as [28, 29]

$$\Psi(z_k, \bar{z}_k) \rightarrow \Psi'(z_k, \bar{z}_k) = (cz_k + d)^{-2s_k} (\bar{c}\bar{z}_k + \bar{d})^{-2\bar{s}_k} \Psi(z'_k, \bar{z}'_k). \quad (2.9)$$

In statistical physics (2.3) is called the Hamiltonian of the non-compact  $\text{SL}(2, \mathbb{C})$  XXX Heisenberg spin magnets. It describes the nearest neighbour interaction between  $N$  non-compact  $\text{SL}(2, \mathbb{C})$  spins attached to the particles with periodic boundary conditions.

For the homogeneous spin chain we have to take  $s_k = s$  and  $\bar{s}_k = \bar{s}$ . In QCD values of  $(s, \bar{s})$  depend on a chosen scalar product in the space of the wave-functions (2.9) and they are usually equal to  $(0, 1)$  or  $(0, 0)$  [27, 19].

### 2.3. Scalar product

In order to find the high energy behaviour of the scattering amplitude we have to solve the Schrödinger equation

$$\mathcal{H}_N^{(s=0, \bar{s}=1)} \Psi(\vec{z}_1, \vec{z}_2, \dots, \vec{z}_N) = E_N \Psi(\vec{z}_1, \vec{z}_2, \dots, \vec{z}_N) \quad (2.10)$$

with the eigenstate  $\Psi(\vec{z}_1, \vec{z}_2, \dots, \vec{z}_N)$  being a single-valued function on the plane  $\vec{z} = (z, \bar{z})$ , normalizable with respect to the  $\text{SL}(2, \mathbb{C})$  invariant scalar product

$$\|\Psi\|^2 = \langle \Psi | \Psi \rangle = \int d^2 z_1 d^2 z_2 \dots d^2 z_N |\Psi(\vec{z}_1, \vec{z}_2, \dots, \vec{z}_N)|^2, \quad (2.11)$$

where  $d^2 z_i = dx_i dy_i = dz_i d\bar{z}_i/2$  with  $\bar{z}_i = z_i^*$ . One may notice that it is possible to use other scalar products corresponding to different choice of  $(s, \bar{s})$ . For farther information see Refs. [17, 21] and [18, 19].

Let us consider the amplitude for the scattering of two colourless objects  $A$  and  $B$ . In the Regge limit, the contribution to the scattering amplitude from  $N$ -gluon exchange in the  $t$ -channel takes the form

$$\mathcal{A}(s, t) = is \sum_N (i\alpha_s)^N \mathcal{A}_N(s, t). \quad (2.12)$$

Using the  $SL(2, \mathbb{C})$  scalar product (2.11) we have

$$\mathcal{A}_N(s, t) = s \int d^2 z_0 e^{i\bar{z}_0 \vec{p}} \langle \tilde{\Phi}_A(\vec{z}_0) | e^{-\bar{\alpha}_s Y \mathcal{H}_N/4} | \tilde{\Phi}_B(0) \rangle, \quad (2.13)$$

where the rapidity  $Y = \ln s$ . Here the Hamiltonian  $\mathcal{H}_N$  is related to the sum of  $N$  BFKL kernels corresponding to nearest neighbour interaction between  $N$  reggeized gluons. The wave-functions  $|\Phi_{A(B)}(\vec{z}_0)\rangle \equiv \Phi_{A(B)}(\vec{z}_i - \vec{z}_0)$  describe the coupling of  $N$ -gluons to the scattered particles. The  $\vec{z}_0$ -integration fixes the momentum transfer  $t = -\vec{p}^2$ .

#### 2.4. Conformal charges $q_k$ and the conformal spins

The Hamiltonian (2.2) possesses a complete set of the integrals of motion  $\{\vec{p}, \vec{q}_k\}$  where  $\vec{q}_k = \{q_k, \bar{q}_k\}$  with  $k = 2, \dots, N$  are called conformal charges while  $\vec{p} = \{p, \bar{p}\}$  is the total momentum of the system. In order to construct them we introduce the Lax operators [30, 31, 32, 33] in holomorphic and anti-holomorphic sectors:

$$\begin{aligned} L_k(u) &= u + i(\sigma \cdot S^{(k)}) = \begin{pmatrix} u + iS_0^{(k)} & iS_-^{(k)} \\ iS_+^{(k)} & u - iS_0^{(k)} \end{pmatrix}, \\ \bar{L}_k(\bar{u}) &= \bar{u} + i(\sigma \cdot \bar{S}^{(k)}) = \begin{pmatrix} \bar{u} + i\bar{S}_0^{(k)} & i\bar{S}_-^{(k)} \\ i\bar{S}_+^{(k)} & \bar{u} - i\bar{S}_0^{(k)} \end{pmatrix} \end{aligned} \quad (2.14)$$

with  $u$  and  $\bar{u}$  being arbitrary complex parameters called the spectral parameters and  $\sigma_\alpha$  being Pauli matrices.

To identify the total set of the integrals of motion of the model, one constructs the auxiliary holomorphic monodromy matrix

$$T_N(u) = L_1(u)L_2(u)\dots L_N(u) \quad (2.15)$$

and similarly for, the anti-holomorphic monodromy operator  $\bar{T}_N(\bar{u})$ . Taking the trace of the monodromy matrix we define the auxiliary transfer matrix (spectral invariants)

$$\hat{t}_N(u) = \text{tr} [T_N(u)] = 2u^N + \hat{q}_2 u^{N-2} + \dots + \hat{q}_N \quad (2.16)$$

and similarly for  $\hat{t}_N(\bar{u})$ . We see from (2.16) the advantage of using the transfer matrix  $\hat{t}_N(u)$ : that is a polynomial in  $u$  with coefficients given in terms of conformal charges  $\hat{q}_k$  and  $\hat{\bar{q}}_k$ , which are expressed as linear combinations of the products of  $k$  spin operators:

$$\begin{aligned}
\hat{q}_2 &= -2 \sum_{i_2 > i_1 = 1}^N \sum_{j_1 = 0}^2 \left( S_{j_1}^{(i_1)} S_{j_1}^{(i_2)} \right) \\
\hat{q}_4 &= - \sum_{i_2 > i_1 = 1}^N \sum_{i_4 > i_3 = 1}^N \sum_{j_1, j_2 = 0}^2 \varepsilon_{i_1 i_2 i_3 i_4} \left( S_{j_1}^{(i_1)} S_{j_1}^{(i_2)} \right) \left( S_{j_2}^{(i_3)} S_{j_2}^{(i_4)} \right) \\
\hat{q}_6 &= -\frac{1}{3} \sum_{i_2 > i_1 = 1}^N \sum_{i_4 > i_3 = 1}^N \sum_{i_6 > i_5 = 1}^N \sum_{j_1, j_2, j_3 = 0}^2 \varepsilon_{i_1 i_2 i_3 i_4 i_5 i_6} \left( S_{j_1}^{(i_1)} S_{j_1}^{(i_2)} \right) \\
&\quad \times \left( S_{j_2}^{(i_3)} S_{j_2}^{(i_4)} \right) \left( S_{j_3}^{(i_5)} S_{j_3}^{(i_6)} \right), \tag{2.17}
\end{aligned}$$

where  $\varepsilon_{i_1 i_2 \dots i_k}$  is completely anti-symmetric tensor and  $\varepsilon_{i_1 i_2 \dots i_k} = 1$  for  $i_1 < i_2 < \dots < i_k$ . So for even  $k$  we have a formula for conformal charges

$$\begin{aligned}
\hat{q}_k &= -\frac{2}{(k/2)!} \sum_{\substack{i_2 > i_1 = 1 \\ i_4 > i_3 = 1 \\ \dots \\ i_n > i_{n-1} = 1}}^N \sum_{j_1, j_2, \dots, j_{k/2} = 0}^2 \varepsilon_{i_1 i_2 \dots i_k} \prod_{n=1}^{k/2} \left( S_{j_n}^{(i_{2n-1})} S_{j_n}^{(i_{2n})} \right). \tag{2.18}
\end{aligned}$$

For odd  $k$ 's we have

$$\begin{aligned}
\hat{q}_3 &= 2 \sum_{i_1, i_2, i_3 = 1}^N \varepsilon_{i_1 i_2 i_3} \left( S_0^{(i_1)} S_1^{(i_2)} S_2^{(i_3)} \right) \\
&= 2 \sum_{i_3 > i_2 > i_1 = 1}^N \sum_{j_1, j_2, j_3 = 0}^2 \varepsilon_{i_1 i_2 i_3} \varepsilon_{j_1 j_2 j_3} \left( S_{j_1}^{(i_1)} S_{j_2}^{(i_2)} S_{j_3}^{(i_3)} \right), \\
\hat{q}_5 &= -2 \sum_{i_3, i_2, i_1 = 1}^N \sum_{i_5 > i_4 = 1}^N \sum_{j_4 = 0}^2 \varepsilon_{i_1 i_2 i_3 i_4 i_5} \left( S_0^{(i_1)} S_1^{(i_2)} S_2^{(i_3)} \right) \left( S_{j_4}^{(i_4)} S_{j_4}^{(i_5)} \right), \\
\hat{q}_7 &= \sum_{i_3, i_2, i_1 = 1}^N \sum_{i_5 > i_4 = 1}^N \sum_{i_7 > i_6 = 1}^N \sum_{j_4, j_5 = 0}^2 \varepsilon_{i_1 i_2 i_3 i_4 i_5 i_6 i_7} \left( S_0^{(i_1)} S_1^{(i_2)} S_2^{(i_3)} \right) \\
&\quad \times \left( S_{j_4}^{(i_4)} S_{j_4}^{(i_5)} \right) \left( S_{j_5}^{(i_6)} S_{j_5}^{(i_7)} \right) \tag{2.19}
\end{aligned}$$

and the general expression for an odd number of the conformal spins is

$$\hat{q}_k = \frac{2(-1)^{(k+1)/2}}{\left(\frac{k-3}{2}\right)!} \sum_{i_3, i_2, i_1=1}^N \sum_{\substack{i_5 > i_4 = 1 \\ i_7 > i_6 = 1 \\ \dots \\ i_k > i_{k-1} = 1}}^N \sum_{j_1, j_2, \dots, j_{(k-3)/2}=0}^2 \varepsilon_{i_1 i_2 \dots i_k} \\ \times \left( S_0^{(i_1)} S_1^{(i_2)} S_2^{(i_3)} \right) \prod_{n=1}^{(k-3)/2} \left( S_{j_n}^{(i_{2n+2})} S_{j_n}^{(i_{2n+3})} \right). \quad (2.20)$$

In the above formulae we have two basic blocks  $\left( S_0^{(i_1)} S_1^{(i_2)} S_2^{(i_3)} \right)$  and  $\left( S_{j_1}^{(i_1)} S_{j_1}^{(i_2)} \right)$  whose products are summed with antisymmetric tensor  $\varepsilon_{i_1 i_2 \dots i_k}$ .

### 2.5. Two-dimensional Lorentz spin and the scaling dimension

The Hamiltonian (2.3) is a function of two-particle Casimir operators [27], and therefore, it commutes with the operators of the total spin  $S_\alpha = \sum_k S_\alpha^{(k)}$  and  $\bar{S}_\alpha = \sum_k \bar{S}_\alpha^{(k)}$ , acting on the quantum space of the system  $V_N \equiv V^{(s_1, \bar{s}_1)} \otimes V^{(s_2, \bar{s}_2)} \otimes \dots \otimes V^{(s_N, \bar{s}_N)}$ . This implies that the eigenstates can be classified according to the irreducible representations of the  $SL(2, \mathbb{C})$  group,  $V^{(h, \bar{h})}$ , parameterized by spins  $(h, \bar{h})$  [27].

The Hamiltonian depends on differences of particle coordinates so the eigenfunctions can be written as

$$\Psi_{\vec{p}}(\vec{z}_1, \vec{z}_2, \dots, \vec{z}_N) = \int d^2 z_0 e^{i\vec{z}_0 \cdot \vec{p}} \Psi(\vec{z}_1 - \vec{z}_0, \vec{z}_2 - \vec{z}_0, \dots, \vec{z}_N - \vec{z}_0). \quad (2.21)$$

The eigenstates  $\Psi(\vec{z}_1, \vec{z}_2, \dots, \vec{z}_N)$  belonging to  $V^{(h, \bar{h})}$  are labelled by the centre-of-mass coordinate  $\vec{z}_0$  and can be chosen to have the following the  $SL(2, \mathbb{C})$  transformation properties

$$\Psi(\{\vec{z}'_k - \vec{z}'_0\}) = \\ = (cz_0 + d)^{2h} (\bar{c}\bar{z}_0 + \bar{d})^{2\bar{h}} \left( \prod_{k=1}^N (cz_k + d)^{2s_k} (\bar{c}\bar{z}_k + \bar{d})^{2\bar{s}_k} \right) \Psi(\{\vec{z}_k - \vec{z}_0\}) \quad (2.22)$$

with  $z_0$  and  $\bar{z}_0$  transforming in the same way as  $z_k$  and  $\bar{z}_k$ , (2.6). As a consequence, they diagonalize the Casimir operators:

$$(S^2 - h(h-1))\Psi(\vec{z}_1, \vec{z}_2, \dots, \vec{z}_N) = 0 \quad (2.23)$$

corresponding to the total spin of the system,

$$S^2 = \sum_{i_2, i_1=1}^N \sum_{j=0}^2 S_j^{(i_1)} S_j^{(i_2)} = -\hat{q}_2 - \sum_{k=1}^N s_k (s_k - 1). \quad (2.24)$$

The complex parameters  $(s_k, \bar{s}_k)$  and  $(h, \bar{h})$  parameterize the irreducible representations of the  $\text{SL}(2, \mathbb{C})$  group. For the principal series representation they satisfy the conditions

$$s_k - \bar{s}_k = n_{s_k}, \quad s_k + (\bar{s}_k)^* = 1 \quad (2.25)$$

and have the following form

$$s_k = \frac{1 + n_{s_k}}{2} + i\nu_{s_k}, \quad \bar{s}_k = \frac{1 - n_{s_k}}{2} + i\nu_{s_k} \quad (2.26)$$

with  $\nu_{s_k}$  being real and  $n_{s_k}$  being integer or half-integer. The spins  $(h, \bar{h})$  are given by similar expressions with  $n_{s_k}$  and  $\nu_{s_k}$  replaced by  $n_h$  and  $\nu_h$ , respectively

$$h = \frac{1 + n_h}{2} + i\nu_h, \quad \bar{h} = \frac{1 - n_h}{2} + i\nu_h. \quad (2.27)$$

The parameter  $n_{s_k}$  has the meaning of the two-dimensional Lorentz spin of the particle, whereas  $\nu_{s_k}$  defines its scaling dimension. To see this one can perform a  $2\pi$ -rotation of the particle on the plane, and find from eigenstates transformations (2.22) that the wave-function acquires a phase. Indeed

$$z_k \rightarrow z_k e^{2\pi i} \text{ and } \bar{z}_k \rightarrow \bar{z}_k e^{-2\pi i} \quad \text{gives} \quad \Psi(z_k, \bar{z}_k) \rightarrow (-1)^{2n_{s_k}} \Psi(z_k, \bar{z}_k). \quad (2.28)$$

For half-integer  $n_{s_k}$  it changes the sign and the corresponding representation is spinorial. Similarly, to define scaling dimension,  $s + \bar{s} = 1 + 2i\nu_{s_k}$  one performs the transformation

$$z \rightarrow \lambda z \quad \text{and} \quad \bar{z} \rightarrow \lambda \bar{z} \quad \text{giving} \quad \Psi(z_k, \bar{z}_k) \rightarrow \lambda^{1+2i\nu_{s_k}} \Psi(z_k, \bar{z}_k). \quad (2.29)$$

Because the scalar product for the wave-functions is invariant under  $\text{SL}(2, \mathbb{C})$  transformations, (2.6), the parameter  $\nu_{s_k}$  is real.

We notice that the holomorphic and anti-holomorphic spin generators as well as Casimir operators (2.5) are conjugated to each other with respect to the scalar product (2.11):

$$[S_\alpha^{(k)}]^\dagger = -\bar{S}_\alpha^{(k)}, \quad [J_k]^\dagger = 1 - \bar{J}_k. \quad (2.30)$$



Moreover, because of the transformation law (2.30),  $h^* = 1 - \bar{h}^{-1}$ . This implies that  $H_N^\dagger = \overline{H}_N$  and, as a consequence, the Hamiltonian is hermitian on the space of the functions endowed with the  $SL(2, \mathbb{C})$  scalar product,  $\mathcal{H}_N^\dagger = \mathcal{H}_N$ .

### 2.6. Conformal charges $\hat{q}_k$ as a differential operators

We noticed in the previous Section that the conformal charge operators  $\hat{q}_k$  are given by invariant sum of linear combinations of the products of  $k$  spin operators. They can be rewritten as  $k$ -th order differential operators acting on (anti)holomorphic coordinates  $(z, \bar{z})$ .

Two particle spin square can be written as

$$\begin{aligned} \sum_{j_1=0}^2 S_{j_1}^{(i_1)} S_{j_1}^{(i_2)} &= \\ &= -\frac{1}{2}(z_{i_1} - z_{i_2})^2 \partial_{z_{i_1}} \partial_{z_{i_2}} + (z_{i_1} - z_{i_2})(s_{i_2} \partial_{z_{i_1}} + s_{i_1} \partial_{z_{i_2}}) + s_1 s_2. \end{aligned} \quad (2.31)$$

For homogeneous spins  $s = s_1 = s_2 = \dots = s_N$ , what is also the QCD case, we have

$$\begin{aligned} \hat{q}_2 &= -2 \sum_{i_2 > i_1 = 1}^N \left( \sum_{j_1=0}^2 S_{j_1}^{(i_1)} S_{j_1}^{(i_2)} \right) \\ &= \sum_{i_2 > i_1 = 1}^N \left( (z_{i_2 i_1})^{2(1-s)} \partial_{z_{i_2}} \partial_{z_{i_1}} (z_{i_2 i_1})^{2s} + 2s(s-1) \right), \\ \hat{q}_3 &= 2 \sum_{i_1, i_2, i_3 = 1}^N \varepsilon_{i_1 i_2 i_3} S_0^{(i_1)} S_1^{(i_2)} S_2^{(i_3)} \\ &= i^3 \sum_{i_3 > i_2 > i_1 = 1}^N \left( z_{i_1 i_2} z_{i_2 i_3} z_{i_3 i_1} \partial_{z_{i_3}} \partial_{z_{i_2}} \partial_{z_{i_1}} + s z_{i_1 i_2} (z_{i_2 i_3} - z_{i_3 i_1}) \partial_{z_{i_2}} \partial_{z_{i_1}} \right. \\ &\quad \left. + s z_{i_2 i_3} (z_{i_3 i_1} - z_{i_1 i_2}) \partial_{z_{i_3}} \partial_{z_{i_2}} + s z_{i_3 i_1} (z_{i_3 i_1} - z_{i_1 i_2}) \partial_{z_{i_3}} \partial_{z_{i_2}} \right. \\ &\quad \left. - 2s^2 z_{i_1 i_2} \partial_{z_{i_3}} - 2s^2 z_{i_2 i_3} \partial_{z_{i_1}} - 2s^2 z_{i_3 i_1} \partial_{z_{i_2}} \right), \end{aligned} \quad (2.32)$$

where  $z_{ij} = z_i - z_j$ . Similar relations hold for the anti-holomorphic sector.

---

<sup>1</sup> \* - denotes complex conjugation

In that way one can also construct operators for the higher conformal charges. They have a particularly simple form for the  $\text{SL}(2, \mathbb{C})$  spins  $s = 0$

$$\hat{q}_k = i^k \sum_{1 \leq j_1 < j_2 < \dots < j_k \leq N} z_{j_1 j_2} \dots z_{j_{k-1}, j_k} z_{j_k, j_1} \partial_{z_{j_1}} \dots \partial_{z_{j_{k-1}}} \partial_{z_{j_k}} \quad (2.33)$$

as well as for  $s = 1$

$$\hat{q}_k = i^k \sum_{1 \leq j_1 < j_2 < \dots < j_k \leq N} \partial_{z_{j_1}} \dots \partial_{z_{j_{k-1}}} \partial_{z_{j_k}} z_{j_1 j_2} \dots z_{j_{k-1}, j_k} z_{j_k, j_1}. \quad (2.34)$$

The eigenvalues of the lowest conformal charge  $\hat{q}_2$  can be parameterized by a conformal weight  $h$  (2.27) and complex spin  $s$  (2.26) as follows

$$q_2 = -h(h-1) + Ns(s-1) \quad (2.35)$$

### 2.7. Other symmetries

The states (2.21) have additional symmetries [27]:

$$\begin{aligned} \mathbb{P} \Psi_{q, \bar{q}}(\vec{z}_1, \vec{z}_2, \dots, \vec{z}_N) &\stackrel{\text{def}}{=} \Psi_{q, \bar{q}}(\vec{z}_2, \vec{z}_3, \dots, \vec{z}_1) \\ &= e^{i\theta_N(q, \bar{q})} \Psi_{q, \bar{q}}(\vec{z}_1, \vec{z}_2, \dots, \vec{z}_N), \\ \mathbb{M} \Psi^\pm(\vec{z}_1, \vec{z}_2, \dots, \vec{z}_N) &\stackrel{\text{def}}{=} \Psi^\pm(\vec{z}_N, \vec{z}_{N-1}, \dots, \vec{z}_1) \\ &= \pm \Psi^\pm(\vec{z}_1, \vec{z}_2, \dots, \vec{z}_N) \end{aligned} \quad (2.36)$$

so called cyclic and mirror permutation where the conformal charges are denoted by  $q \equiv (q_2, q_3, \dots, q_n)$  and  $\bar{q} \equiv (\bar{q}_2, \bar{q}_3, \dots, \bar{q}_n)$ . The generators  $\mathbb{P}$  and  $\mathbb{M}$ , respectively, commute with the Hamiltonian  $\mathcal{H}$  but they do not commute with each other. They satisfy relations

$$\mathbb{P}^N = \mathbb{M}^2 = 1, \quad \mathbb{P}^\dagger = \mathbb{P}^{-1} = \mathbb{P}^{N-1}, \quad \mathbb{M}^\dagger = \mathbb{M}, \quad \mathbb{P}\mathbb{M} = \mathbb{M}\mathbb{P}^{-1} = \mathbb{M}\mathbb{P}^{N-1}. \quad (2.37)$$

The phase  $\theta_N(q)$  which is connected with eigenvalues of  $\mathbb{P}$  is called quasi-momentum. It takes the following values

$$\theta_N(q, \bar{q}) = 2\pi \frac{k}{N}, \quad \text{for } k = 0, 1, \dots, N-1. \quad (2.38)$$

The eigenstates of the conformal charges  $\hat{q}_k$  diagonalize  $\mathcal{H}$  and  $\mathbb{P}$ .

The transfer matrices (2.16) are invariant under the cyclic permutations  $\mathbb{P}^\dagger \hat{t}_N(u) \mathbb{P} = \hat{t}_N(u)$  whereas they transform under the mirror transformation as

$$\mathbb{M} \hat{t}_N(u) \mathbb{M} = (-1)^N \hat{t}_N(-u). \quad (2.39)$$

Substituting (2.16) into (2.39) one derives a transformation law of the conformal charges  $q_k$

$$\mathbb{P}^\dagger \hat{q}_k \mathbb{P} = \hat{q}_k \quad \mathbb{M} \hat{q}_k \mathbb{M} = (-1)^k \hat{q}_k \quad (2.40)$$

and similarly for the anti-holomorphic charges. Since the Hamiltonian (2.3) is invariant under the mirror permutation, it has to satisfy

$$\mathcal{H}(\hat{q}_k, \hat{\bar{q}}_k) = \mathbb{M} \mathcal{H}(\hat{q}_k, \hat{\bar{q}}_k) \mathbb{M} = \mathcal{H}(\mathbb{M} \hat{q}_k \mathbb{M}, \mathbb{M} \hat{\bar{q}}_k \mathbb{M}) = \mathcal{H}((-1)^k \hat{q}_k, (-1)^k \hat{\bar{q}}_k). \quad (2.41)$$

This implies that the eigenstates of the Hamiltonian (2.3) corresponding to two different sets of the quantum number  $\{q_k, \bar{q}_k\}$  and  $\{(-1)^k q_k, (-1)^k \bar{q}_k\}$  have the same energy

$$E_N(q_k, \bar{q}_k) = E_N((-1)^k q_k, (-1)^k \bar{q}_k). \quad (2.42)$$

Similarly one can derive relation for quasimomentum

$$\theta_N(q_k, \bar{q}_k) = -\theta_N((-1)^k q_k, (-1)^k \bar{q}_k). \quad (2.43)$$

The cyclic and mirror permutation symmetries come from the Bose symmetry and they appear after performing the multi-colour limit [23]. Physical states should possess both symmetries.

### 3. Baxter Q-operator

#### 3.1. Definition of the Baxter Q-operator

The Schrödinger equation (2.10) may be solved applying the powerful method of the Baxter Q-operator [26]. It depends on two complex spectral parameters  $u, \bar{u}$  and in the following will be denoted as  $\mathbb{Q}(u, \bar{u})$ . This operator has to satisfy the following relations

- Commutativity:

$$[\mathbb{Q}(u, \bar{u}), \mathbb{Q}(v, \bar{v})] = 0, \quad (3.1)$$

- $Q - t$  relation:

$$[\hat{t}_N(u), \mathbb{Q}(u, \bar{u})] = [\hat{t}_N(\bar{u}), \mathbb{Q}(u, \bar{u})] = 0, \quad (3.2)$$

- Baxter equation:

$$\hat{t}_N(u) \mathbb{Q}(u, \bar{u}) = (u + is)^N \mathbb{Q}(u + i, \bar{u}) + (u - is)^N \mathbb{Q}(u - i, \bar{u}), \quad (3.3)$$

$$\hat{t}_N(\bar{u}) \mathbb{Q}(u, \bar{u}) = (\bar{u} + i\bar{s})^N \mathbb{Q}(u, \bar{u} + i) + (\bar{u} - i\bar{s})^N \mathbb{Q}(u, \bar{u} - i), \quad (3.4)$$

where  $\hat{t}_N(u)$  and  $\hat{t}_N(\bar{u})$  are the auxiliary transfer matrices (2.16). According to (3.2) the Baxter  $\mathbb{Q}(u, \bar{u})$ -operator and the auxiliary transfer matrices as well as the Hamiltonian (2.2) share the common set of the eigenfunctions

$$\mathbb{Q}(u, \bar{u})\Psi_{q, \bar{q}}(\vec{z}_1, \vec{z}_2, \dots, \vec{z}_N) = Q_{q, \bar{q}}(u, \bar{u})\Psi_{q, \bar{q}}(\vec{z}_1, \vec{z}_2, \dots, \vec{z}_N). \quad (3.5)$$

The eigenvalues of the  $Q$ -operator satisfy the same Baxter equation (3.3) and (3.4) with the auxiliary transfer matrices replaced by their corresponding eigenvalues.

In the paper [27] the  $Q$ -operator was constructed as an  $N$ -fold integral operator

$$\mathbb{Q}(u, \bar{u})\Psi(\vec{z}_1, \vec{z}_2, \dots, \vec{z}_N) = \int d^2w_1 \int d^2w_2 \dots \int d^2w_N Q_{u, \bar{u}}(\vec{z}_1, \vec{z}_2, \dots, \vec{z}_N | \vec{w}_1, \vec{w}_2, \dots, \vec{w}_N) \Psi(\vec{w}_1, \vec{w}_2, \dots, \vec{w}_N), \quad (3.6)$$

where the integrations are performed over two-dimensional  $\vec{w}_i$ -planes. The integral kernel in (3.6) takes two different forms:

$$\begin{aligned} Q_{u, \bar{u}}^{(+)}(\vec{z} | \vec{w}) &= \\ &= a(2 - 2s, s + iu, \bar{s} - i\bar{u})^N \pi^N \prod_{k=1}^N \frac{[z_k - z_{k+1}]^{1-2s}}{[w_k - z_k]^{1-s-iu} [w_k - z_{k+1}]^{1-s+iu}} \end{aligned} \quad (3.7)$$

and

$$Q_{u, \bar{u}}^{(-)}(\vec{z} | \vec{w}) = \prod_{k=1}^N \frac{[w_k - w_{k+1}]^{2s-2}}{[z_k - w_k]^{s+iu} [z_k - w_{k+1}]^{s-iu}}, \quad (3.8)$$

which appear to be equivalent [27]. In Eqs. (3.7) and (3.8) function  $a(\dots)$  factorizes as

$$a(\alpha, \beta, \dots) = a(\alpha)a(\beta) \dots \quad \text{and} \quad a(\alpha) = \frac{\Gamma(1 - \bar{\alpha})}{\Gamma(\alpha)} \quad (3.9)$$

and  $\bar{\alpha}$  is an anti-holomorphic partner of  $\alpha$  satisfying  $\alpha - \bar{\alpha} \in \mathbb{Z}$ . Moreover, the two-dimensional propagators are defined as

$$[z_k - w_k]^{-\alpha} = (z_k - w_k)^{-\alpha} (\bar{z}_k - \bar{w}_k)^{-\bar{\alpha}}. \quad (3.10)$$

In order for the Baxter  $Q$ -operators to be well defined, (3.7) and (3.8), should be single-valued functions. In this way we can find that the spectral parameters  $u$  and  $\bar{u}$  have to satisfy the condition

$$i(u - \bar{u}) = n \quad (3.11)$$

with  $n$  being an integer.

The Baxter  $Q$ -operator has a well defined pole structure. For  $\mathbb{Q}^{(+)}(u, \bar{u})$  we have an infinite set of poles of the order not higher than  $N$  situated at

$$\left\{ u_m^+ = i(s - m), \bar{u}_m^+ = i(\bar{s} - \bar{m}) \right\}; \quad \left\{ u_m^- = -i(s - m), \bar{u}_m^- = -i(\bar{s} - \bar{m}) \right\} \quad (3.12)$$

with  $m, \bar{m} = 1, 2, \dots$ . The behaviour of  $Q_{q, \bar{q}}(u, \bar{u}) \equiv Q_{q, \bar{q}}^{(+)}(u, \bar{u})$  *i.e.* an eigenvalue of  $\mathbb{Q}^{(+)}(u, \bar{u})$ , in the vicinity of the pole at  $m = \bar{m} = 1$  can be parameterized as

$$Q_{q, \bar{q}}(u_1^\pm + \epsilon, \bar{u}_1^\pm + \epsilon) = R^\pm(q, \bar{q}) \left[ \frac{1}{\epsilon^N} + \frac{i E^\pm(q, \bar{q})}{\epsilon^{N-1}} + \dots \right]. \quad (3.13)$$

The functions  $R^\pm(q, \bar{q})$  fix an overall normalization of the Baxter operator, while the residue functions  $E^\pm(q, \bar{q})$  define the energy of the system (see Eqs. (3.21) and (3.24) below). It has also specified asymptotic behaviour. For  $|\text{Im}\lambda| < 1/2$  and  $\text{Re}\lambda \rightarrow \infty$

$$Q_{q, \bar{q}}(\lambda - in/2, \lambda + in/2) \sim e^{i\Theta_h(q, \bar{q})} \lambda^{h+\bar{h}-N(s-\bar{s})} + e^{-i\Theta_h(q, \bar{q})} \lambda^{1-h+1-\bar{h}-N(s-\bar{s})}, \quad (3.14)$$

where  $\Theta_h$  is a phase that should not be confused with quasimomentum  $\theta_N(q, \bar{q})$ .

### 3.2. Observables

The Hamiltonian (2.2) may be written in terms of the Baxter  $Q$ -operator [27]:

$$\mathcal{H}_N = \epsilon_N + i \frac{d}{du} \ln \mathbb{Q}^{(+)}(u + is, \bar{u} + i\bar{s}) \Big|_{u=0} - \left( i \frac{d}{du} \ln \mathbb{Q}^{(+)}(u - is, \bar{u} - i\bar{s}) \Big|_{u=0} \right)^\dagger, \quad (3.15)$$

where the additive normalization constant is given as

$$\epsilon_N = 2N \text{Re}[\psi(2s) + \psi(2 - 2s) - 2\psi(1)]. \quad (3.16)$$

Applying to (3.15) the eigenstate  $\Psi_q$  we obtain the energy

$$E_N(q, \bar{q}) = \epsilon_N + i \frac{d}{du} \ln [Q_{q, \bar{q}}(u + is, u + i\bar{s}) (Q_{q, \bar{q}}(u - is, u - i\bar{s}))^*] \Big|_{u=0}, \quad (3.17)$$

or equivalently

$$E_N(q, \bar{q}) = -\text{Im} \frac{d}{du} \ln \left[ u^{2N} Q_{q, \bar{q}}(u + i(1-s), u + i(1-\bar{s})) \right. \\ \left. \times Q_{-q, -\bar{q}}(u + i(1-s), u + i(1-\bar{s})) \right] \Big|_{u=0}, \quad (3.18)$$

where  $Q_{q, \bar{q}}(u, \bar{u}) \equiv Q_{q, \bar{q}}^{(+)}(u, \bar{u})$  is eigenvalue of the  $\mathbb{Q}^{(+)}(u, \bar{u})$  operator, while

$$\pm q = (q_2, \pm q_3, \dots, (\pm)^N q_N) \quad (3.19)$$

are the conformal charges.

It is also possible to rewrite the quasimomentum operator in terms of  $\mathbb{Q}_+(u, \bar{u})$ :

$$\hat{\theta}_N = -i \ln \mathbb{P} = i \ln \frac{\mathbb{Q}_+(is, i\bar{s})}{\mathbb{Q}_+(-is, -i\bar{s})}. \quad (3.20)$$

Moreover, using the mirror permutation (2.40) one finds the following parity relations for the residue functions  $R^+(q, \bar{q})$  defined in (3.13):

$$R^+(q, \bar{q})/R^+(-q, -\bar{q}) = e^{2i\theta_N(q, \bar{q})} \quad (3.21)$$

and for the eigenvalues of the Baxter operator:

$$Q_{q, \bar{q}}(-u, -\bar{u}) = e^{i\theta_N(q, \bar{q})} Q_{-q, -\bar{q}}(u, \bar{u}), \quad (3.22)$$

where  $-q \equiv (q_2, -q_3, \dots, (-1)^n q_n)$  and similarly for  $\bar{q}$ . Examining the behaviour of (3.22) around the pole at  $u = u_1^\pm$  and  $\bar{u} = \bar{u}_1^\pm$  and making use of Eq. (3.13) one gets

$$R^\pm(q, \bar{q}) = (-1)^N e^{i\theta_N(q, \bar{q})} R^\mp(-q, -\bar{q}), \quad E^\pm(q, \bar{q}) = -E^\mp(-q, -\bar{q}). \quad (3.23)$$

To obtain the expression for the energy  $E_N(q, \bar{q})$ , we apply (3.17) and replace the function  $Q_{q, \bar{q}}(u \pm i(1-s), u \pm i(1-\bar{s}))$  by its pole expansion (3.13). Then, applying the second relation in (3.23), one finds

$$E_N(q, \bar{q}) = E^+(-q, -\bar{q}) + (E^+(q, \bar{q}))^* = \text{Re} [E^+(-q, -\bar{q}) + E^+(q, \bar{q})], \quad (3.24)$$

where the last relation follows from hermiticity of the Hamiltonian (2.3). We conclude from Eqs. (3.24) and (3.13), that in order to find the energy  $E_N(q, \bar{q})$ , one has to calculate the residue of  $Q_{q, \bar{q}}(u, \bar{u})$  at the  $(N-1)$ -th order pole at  $u = i(s-1)$  and  $\bar{u} = i(\bar{s}-1)$ .

### 3.3. Construction of the eigenfunction

The Hamiltonian eigenstate  $\Psi_{\vec{p},\{q,\bar{q}\}}(\vec{z})$  is a common eigenstate of the total set of the integrals of motion,  $\vec{p}$  and  $\{q,\bar{q}\}$  as well as the Baxter  $Q$ -operator. Thanks to the method of the Separation of Variables (SoV) developed by Sklyanin [30, 27] we can write the eigenstate using separated coordinates  $\vec{x} = (\vec{x}_1, \dots, \vec{x}_{N-1})$  as

$$\Psi_{\vec{p},\{q,\bar{q}\}}(\vec{z}) = \int d^{N-1}\vec{x} \mu(\vec{x}_1, \dots, \vec{x}_{N-1}) U_{\vec{p},\vec{x}_1, \dots, \vec{x}_{N-1}}(\vec{z}_1, \dots, \vec{z}_N) \times (\Phi_{q,\bar{q}}(\vec{x}_1, \dots, \vec{x}_{N-1}))^*, \quad (3.25)$$

where  $U_{\vec{p},\vec{x}}$  is the kernel of the unitary operator while

$$\begin{aligned} & (\Phi_{q,\bar{q}}(\vec{x}_1, \dots, \vec{x}_{N-1}))^* = \\ & = e^{i\theta_N(q,\bar{q})/2} \prod_{k=1}^{N-1} \left( \frac{\Gamma(s + ix_k)\Gamma(\bar{s} - i\bar{x}_k)}{\Gamma(1 - s + ix_k)\Gamma(1 - \bar{s} - i\bar{x}_k)} \right)^N Q_{q,\bar{q}}(x_k, \bar{x}_k). \end{aligned} \quad (3.26)$$

The functions  $Q_{q,\bar{q}}(x_k, \bar{x}_k)$  are eigenstates of the Baxter  $Q$ -operator. In contrast to the  $\vec{z}_i = (z_i, \bar{z}_i)$  - coordinates, the allowed values of separated coordinates are

$$x_k = \nu_k - \frac{in_k}{2}, \quad \bar{x}_k = \nu_k + \frac{in_k}{2} \quad (3.27)$$

with  $n_k$  integer and  $\nu_k$  real. Integration over the space of separated variables implies summation over integer  $n_k$  and integration over continuous  $\nu_k$

$$\int d^{N-1}\vec{x} = \prod_{k=1}^{N-1} \left( \sum_{n_k=-\infty}^{\infty} \int_{-\infty}^{\infty} d\nu_k \right), \quad \mu(\vec{x}) = \frac{2\pi^{-N^2}}{(N-1)!} \prod_{\substack{j,k=1 \\ j>k}}^{N-1} |\vec{x}_k - \vec{x}_j|^2, \quad (3.28)$$

where  $|\vec{x}_k - \vec{x}_j|^2 = (\nu_k - \nu_j)^2 + (n_k - n_j)^2/4$ .

The integral kernel  $U_{\vec{p},\vec{x}}$  can be written as

$$U_{\vec{p},\vec{x}}(\vec{z}_1, \dots, \vec{z}_N) = c_N(\vec{x})(\vec{p}^2)^{(N-1)/2} \int d^2 w_N e^{2i\vec{p} \cdot \vec{w}_N} U_{\vec{x}}(\vec{z}_1, \dots, \vec{z}_N; \vec{w}_N), \quad (3.29)$$

where  $2\vec{p} \cdot \vec{w}_N = p w_N + \bar{p} \bar{w}_N$ ,

$$U_{\vec{x}}(\vec{z}_1, \dots, \vec{z}_N; \vec{w}_N) = \left[ \Lambda_{N-1,(\vec{x}_1)}^{(s,\bar{s})} \Lambda_{N-2,(\vec{x}_2)}^{(1-s,1-\bar{s})} \dots \Lambda_{1,(\vec{x}_{N-1})}^{(s,\bar{s})} \right] (\vec{z}_1, \dots, \vec{z}_N | \vec{w}_N) \quad (3.30)$$

for even  $N$ , and

$$U_{\vec{x}}(\vec{z}_1, \dots, \vec{z}_N; \vec{w}_N) = \left[ \Lambda_{N-1, (\vec{x}_1)}^{(s, \bar{s})} \Lambda_{N-2, (\vec{x}_2)}^{(1-s, 1-\bar{s})} \cdots \Lambda_{1, (\vec{x}_{N-1})}^{(1-s, 1-\bar{s})} \right] (\vec{z}_1, \dots, \vec{z}_N | \vec{w}_N) \quad (3.31)$$

for odd  $N$ . Here the convolution involves the product of  $(N-1)$  functions  $\Lambda_{N-k, (\vec{x}_k)}$  with alternating spins  $(s, \bar{s})$  and  $(1-s, 1-\bar{s})$ . They are defined as

$$\Lambda_{N-n, (\vec{x})}^{(s, \bar{s})}(\vec{z}_n, \dots, \vec{z}_N | \vec{y}_{n+1}, \dots, \vec{y}_N) = [z_1 - y_2]^{-x+iu} \\ \times \left( \prod_{k=n+1}^{N-1} [z_k - y_k]^{-x-iu} [z_k - y_{k+1}]^{-x+iu} \right) [z_N - y_N]^{-x-iu}, \quad (3.32)$$

where the convolution  $[\Lambda_{N-k, (\vec{x}_k)} \Lambda_{N-k+1, (\vec{x}_{k-1})}]$  contains  $(N-k)$  two-dimensional integrals. The coefficient  $c_N(\vec{x})$  is given for  $N \geq 3$

$$c_N(\vec{x}) = \prod_{k=1}^{[(N-1)/2]} (a(s + ix_{2k}, \bar{s} - i\bar{x}_{2k}))^{N-k} \\ \times \prod_{k=1}^{[N/2-1]} (a(s + ix_{2k+1}, \bar{s} - i\bar{x}_{2k+1}))^k \quad (3.33)$$

while the products go over integer numbers lower than upper limit. For  $N=2$  we have  $c_2(\vec{x}_1) = 1$ .

#### 4. Quantization conditions in the $Q$ -Baxter method

In Ref. [17] the authors describe a construction of the solution to the Baxter equations, (3.3) and (3.4), which satisfies additionally the conditions (3.12) and (3.14). This can be done by means of the following integral representation for  $Q_{q, \bar{q}}(u, \bar{u})$

$$Q_{q, \bar{q}}(u, \bar{u}) = \int \frac{d^2 z}{z \bar{z}} z^{-iu} \bar{z}^{-i\bar{u}} Q(z, \bar{z}), \quad (4.1)$$

where we integrate over the two-dimensional  $\vec{z}$ -plane with  $\bar{z} = z^*$  and  $Q(z, \bar{z})$  depends on  $\{q, \bar{q}\}$ . The advantages of this ansatz are:

- the functional Baxter equation on  $Q_{q, \bar{q}}(u, \bar{u})$  is transformed into the



$N$ -th order differential equation for the function  $Q(z, \bar{z})$

$$\left[ z^s (z\partial_z)^N z^{1-s} + z^{-s} (z\partial_z)^N z^{s-1} - 2(z\partial_z)^N - \sum_{k=2}^N i^k q_k (z\partial_z)^{N-k} \right] Q(z, \bar{z}) = 0. \quad (4.2)$$

A similar equation holds in the anti-holomorphic sector with  $s$  and  $q_k$  replaced by  $\bar{s} = 1 - s^*$  and  $\bar{q}_k = q_k^*$ , respectively.

- the condition (3.11) is automatically satisfied since the  $z$ -integral in the r.h.s. of (4.1) is well-defined only for  $i(u - \bar{u}) = n$ .
- the remaining two conditions for the analytical properties and asymptotic behaviour of  $Q_{q, \bar{q}}(u, \bar{u})$ , Eqs. (3.12) and (3.14), become equivalent to the requirement for  $Q(z, \bar{z} = z^*)$  to be a single-valued function on the complex  $z$ -plane.

The differential equation (4.2) is of Fuchsian type. It possesses three regular singular points located at  $z = 0$ ,  $z = 1$  and  $z = \infty$ . Moreover, it has  $N$  linearly independent solutions,  $Q_a(z)$ . The anti-holomorphic equation has also  $N$  independent solutions,  $\bar{Q}_b(\bar{z})$ .

Now, we construct the general expression for the function  $Q(z, \bar{z})$  as

$$Q(z, \bar{z}) = \sum_{a,b=1}^N Q_a(z) C_{ab} \bar{Q}_b(\bar{z}), \quad (4.3)$$

where  $C_{ab}$  is an arbitrary mixing matrix. The functions  $Q_a(z)$  and  $\bar{Q}_b(\bar{z})$  have a nontrivial monodromy<sup>2</sup> around three singular points,  $z, \bar{z} = 0, 1$  and  $\infty$ . In order to be well-defined on the whole plane, functions  $Q(z, \bar{z} = z^*)$  should be single-valued and their monodromy should cancel in the r.h.s. of (4.3). This condition allows us to determine the values of the mixing coefficients,  $C_{ab}$ , and also to calculate the quantized values of the conformal charges  $q_k$ .

The differential equation (4.2) is also symmetric under the transformation  $z \rightarrow 1/z$  and  $q_k \rightarrow (-1)^k q_k$ . This property is related to Eq. (3.22) and leads to

$$Q_{q, \bar{q}}(z, \bar{z}) = e^{i\theta_N(q, \bar{q})} Q_{-q, -\bar{q}}(1/z, 1/\bar{z}), \quad (4.4)$$

---

<sup>2</sup> The monodromy matrix around  $z = 0$  is defined as  $Q_n^{(0)}(z e^{2\pi i}) = M_{nk} Q_k^{(0)}(z)$  and similarly for the other singular points.

where  $\pm q = (q_2, \pm q_3, \dots, (\pm)^N q_N)$  denotes the integrals of motion corresponding to the function  $Q(z, \bar{z})$ . The above formula allows us to define the solution  $Q(z, \bar{z})$  around  $z = \infty$  from the solution at  $z = 0$ . Thus, applying (4.4) we are able to find  $Q(z, \bar{z})$  and analytically continue it to the whole  $z$ -plane.

#### 4.1. Solution around $z = 0$

We find a solution  $Q(z) \sim z^a$  by the series method. The indicial equation for the solution of Eq. (4.2) around  $z = 0$  reads as follows

$$(a - 1 + s)^N = 0 \quad (4.5)$$

and the solution,  $a = 1 - s$  is  $N$ -fold degenerate. This leads to terms  $\sim \text{Log}^k(z)$  with  $k \leq N - 1$ . We define the fundamental set of linearly independent solutions to (4.2) around  $z = 0$  as

$$\begin{aligned} Q_1^{(0)}(z) &= z^{1-s} u_1(z), \\ Q_m^{(0)}(z) &= z^{1-s} \left[ u_1(z) \text{Log}^{m-1}(z) \right. \\ &\quad \left. + \sum_{k=1}^{m-1} c_{m-1}^k u_{k+1}(z) \text{Log}^{m-k-1}(z) \right], \end{aligned} \quad (4.6)$$

with  $2 \leq m \leq N$  and where for the later convenience

$$c_{m-1}^k = \frac{(m-1)!}{(k!(m-k-1)!)}. \quad (4.7)$$

The functions  $u_m(z)$  are defined inside the region  $|z| < 1$  and have a form

$$u_m(z) = 1 + \sum_{n=1}^{\infty} z^n u_n^{(m)}(q). \quad (4.8)$$

Inserting (4.6) and (4.8) into (4.2), one derives recurrence relations for  $u_n^{(m)}(q)$ . However, in order to save space, we do not show here their explicit form.

In the anti-holomorphic sector the fundamental set of solutions can be obtained from (4.6) by substituting  $s$  and  $q_k$  by  $\bar{s} = 1 - s^*$  and  $\bar{q}_k = q_k^*$ , respectively. Sewing the two sectors we obtain the general solution for  $Q(z, \bar{z})$  around  $z = 0$  as

$$Q(z, \bar{z}) \stackrel{|z| \rightarrow 0}{=} \sum_{m, \bar{m}=1}^N Q_m^{(0)}(z) C_{m\bar{m}}^{(0)} \bar{Q}_{\bar{m}}^{(0)}(\bar{z}). \quad (4.9)$$

The above solution (4.9) should be single-valued on the  $z$ -plane. Thus, imposing single-valuedness condition on (4.9) we find a structure of the mixing matrix  $C_{m\bar{m}}^{(0)}$  which for  $n + m \leq N + 1$

$$C_{nm}^{(0)} = \frac{\sigma}{(n-1)!(m-1)!} \sum_{k=0}^{N-n-m+1} \frac{(-2)^k}{k!} \alpha_{k+n+m-1} \quad (4.10)$$

with  $\sigma, \alpha_1, \dots, \alpha_{N-1}$  being arbitrary complex parameters and  $\alpha_N = 1$ . Below the main anti-diagonal, that is for  $n + m > N + 1$ ,  $C_{nm}^{(0)}$  vanish.

The mixing matrix  $C_{m\bar{m}}^{(0)}$  depends on  $N$  arbitrary complex parameters  $\sigma$  and  $\alpha_k$ . However, two parity relations, Eqs. (3.21) and (4.4), fix  $\sigma = \exp(i\theta_N(q, \bar{q}))$ , with  $\theta_N(q, \bar{q})$  being the quasimomentum, and lead to the quantization of the quasimomentum. Later, we will use (4.4) to calculate the eigenvalues of  $\theta_N(q, \bar{q})$  (see Eq. (4.25)).

The leading asymptotic behaviour of  $Q(z, \bar{z})$  for  $z \rightarrow 0$  can be obtained by substituting (4.10) and (4.6) into (4.9). It has a form

$$Q_{q, \bar{q}}(z, \bar{z}) = z^{1-s} \bar{z}^{1-\bar{s}} e^{i\theta_N(q, \bar{q})} \left[ \frac{\text{Log}^{N-1}(z\bar{z})}{(N-1)!} + \frac{\text{Log}^{N-2}(z\bar{z})}{(N-2)!} \alpha_{N-1} + \dots + \frac{\text{Log}(z\bar{z})}{1!} \alpha_2 + \alpha_1 \right] (1 + \mathcal{O}(z, \bar{z})). \quad (4.11)$$

Making use of the integral identity

$$\int_{|z|<\rho} \frac{d^2z}{z\bar{z}} z^{-iu} \bar{z}^{-i\bar{u}} \ln^n(z\bar{z}) z^{m-s} \bar{z}^{\bar{m}-\bar{s}} = \pi \delta_{m-s-iu, \bar{m}-\bar{s}-i\bar{u}} \left[ \frac{(-1)^n n!}{(m-s-iu)^{n+1}} + \mathcal{O}((m-s-iu)^0) \right], \quad (4.12)$$

with  $m$  and  $\bar{m}$  positive integer, we can calculate the contribution of the small- $z$  region to the eigenvalue of the Baxter equation (4.1). The function  $Q_{q, \bar{q}}(u, \bar{u})$  has poles of the order  $N$  in the points  $u = i(s-m)$  and  $\bar{u} = i(\bar{s}-\bar{m})$  what agrees with (3.12). For  $m = \bar{m} = 1$  one finds from (4.11)

$$Q_{q, \bar{q}}(u_1^+ + \epsilon, \bar{u}_1^+ + \epsilon) = -\frac{\pi e^{i\theta_N(q, \bar{q})}}{(i\epsilon)^N} \left[ 1 + i\epsilon \alpha_{N-1} + \dots + (i\epsilon)^{N-2} \alpha_2 + (i\epsilon)^{N-1} \alpha_1 + \mathcal{O}(\epsilon^N) \right], \quad (4.13)$$

where  $u_1^+$  and  $\bar{u}_1^+$  are defined in (3.12). One can see that the integration in (4.1) over the region of large  $z$  with (4.4) and (4.11) gives the second set of poles for  $Q_{q, \bar{q}}(u, \bar{u})$  located at  $u = -i(s-m)$  and  $\bar{u} = -i(\bar{s}-\bar{m})$ .

Comparing (4.13) with (3.13) one obtains

$$R^+(q, \bar{q}) = -\frac{\pi}{i^N} e^{i\theta_N(q, \bar{q})}, \quad E^+(q, \bar{q}) = \alpha_{N-1}(q, \bar{q}). \quad (4.14)$$

Now, we may derive expression for the energy

$$E_N(q, \bar{q}) = \text{Re}[\alpha_{N-1}(-q, -\bar{q}) + \alpha_{N-1}(q, \bar{q})]. \quad (4.15)$$

The arbitrary complex parameters  $\alpha_n$ , defined in (4.10), will be fixed by the quantization conditions below.

In this Section we have obtained following Ref. [17] the expression for the energy spectrum  $E_N(q, \bar{q})$ , as a function of the matrix elements of the mixing matrix (4.10) in the fundamental basis (4.6). Moreover, we have defined the solution to the Baxter equation  $Q(u, \bar{u})$  and reproduced the analytical properties of the eigenvalues of the Baxter operator, Eq. (3.12).

#### 4.2. Solution around $z = 1$

Looking for a solution of (4.2) around  $z = 1$  in a form  $Q(z) \sim (z - 1)^b$  we obtain the following indicial equation

$$(b + 1 + h - Ns)(b + 2 - h - Ns) \prod_{k=0}^{N-3} (b - k) = 0, \quad (4.16)$$

where  $h$  is the total  $\text{SL}(2, \mathbb{C})$  spin defined in (2.35). Although the solutions  $b = k$  with  $k = 0, \dots, N - 3$  differ from each other by an integer, for  $h \neq (1 + n_h)/2$ , no logarithmic terms appear. The  $\text{Log}(z)$ -terms are only needed for  $\text{Im}h = 0$  where the additional degeneration occurs.

Thus, we define the fundamental set of solutions to Eq. (4.2) around  $z = 1$ . For  $\text{Im}h \neq 0$  it has the form

$$\begin{aligned} Q_1^{(1)}(z) &= z^{1-s}(1-z)^{Ns-h-1}v_1(z), \\ Q_2^{(1)}(z) &= z^{1-s}(1-z)^{Ns+h-2}v_2(z), \\ Q_m^{(1)}(z) &= z^{1-s}(1-z)^{m-3}v_m(z), \end{aligned} \quad (4.17)$$

with  $m = 3, \dots, N$ . The functions  $v_i(z)$  ( $i = 1, 2$ ) and  $v_m(z)$  given by the power series

$$v_i(z) = 1 + \sum_{n=1}^{\infty} (1-z)^n v_n^{(i)}(q), \quad v_m(z) = 1 + \sum_{n=N-m+1}^{\infty} (1-z)^n v_n^{(m)}(q), \quad (4.18)$$

which converge inside the region  $|1 - z| < 1$  and where the expansion coefficients  $v_n^{(i)}$  and  $v_n^{(m)}$  satisfy the  $N$ -term recurrence relations<sup>3</sup> with respect to the index  $n$ . For  $h = (1 + n_h)/2 \in 2\mathbb{Z} + 1$ , one  $\text{Log}(z)$ -terms appear so for  $n_h \geq 0$ ,

$$Q_1^{(1)}(z) \Big|_{h=(1+n_h)/2} = z^{1-s}(1-z)^{Ns-(n_h+3)/2} [(1-z)^{n_h} \text{Log}(1-z) v_2(z) + \tilde{v}_1(z)] , \quad (4.19)$$

where the function  $v_2(z)$  is the same as before,  $\tilde{v}_1(z) = \sum_{k=0}^{\infty} \tilde{v}_k z^k$  and the coefficients  $\tilde{v}_k$  satisfy recurrence relations with the boundary condition  $\tilde{v}_{n_h} = 1$ . For  $h \in \mathbb{Z}$  we have two additional terms:  $\text{Log}(z)$  and  $\text{Log}^2(z)$ .

Similar calculations have to be performed in the anti-holomorphic sector with  $s$  and  $h$  replaced by  $\bar{s} = 1 - s^*$  and  $\bar{h} = 1 - h^*$ , respectively. A general solution for  $Q(z, \bar{z})$  for  $\text{Im}(h) \neq 0$  with respect to the single-valuedness can be constructed as

$$Q(z, \bar{z}) \stackrel{|z| \rightarrow 1}{=} \beta_h Q_1^{(1)}(z) \bar{Q}_1^{(1)}(\bar{z}) + \beta_{1-h} Q_2^{(1)}(z) \bar{Q}_2^{(1)}(\bar{z}) + \sum_{m, \bar{m}=3}^N Q_m^{(1)}(z) \gamma_{m\bar{m}} \bar{Q}_{\bar{m}}^{(1)}(\bar{z}) . \quad (4.20)$$

Here the parameters  $\beta_h$  and  $\gamma_{m\bar{m}}$  build the  $C^{(1)}$  matrix where  $Q(z, \bar{z}) = Q_m^{(1)} C_{m\bar{m}}^{(1)} \bar{Q}_{\bar{m}}^{(1)}$ . The  $\beta$ -coefficients depend, in general, on the total spin  $h$  (and  $\bar{h} = 1 - h^*$ ). They are chosen in (4.20) in such a way that the symmetry of the eigenvalues of the Baxter operator under  $h \rightarrow 1 - h$  becomes manifest. Thus, the mixing matrix  $C^{(1)}$  defined in (4.20) depends on  $2 + (N - 2)^2$  complex parameters  $\beta_h, \beta_{1-h}$  and  $\gamma_{m\bar{m}}$  which are some functions of the integrals of motion  $(q, \bar{q})$ , so, they can be fixed by the quantization conditions.

For  $h = (1 + n_h)/2$  the first two terms in the r.h.s. of (4.20) look differently in virtue of (4.19)

$$Q(z, \bar{z}) \Big|_{h=(1+n_h)/2} = \beta_1 \left[ Q_1^{(1)}(z) \bar{Q}_2^{(1)}(\bar{z}) + Q_2^{(1)}(z) \bar{Q}_1^{(1)}(\bar{z}) \right] + \beta_2 Q_2^{(1)}(z) \bar{Q}_2^{(1)}(\bar{z}) + \dots , \quad (4.21)$$

where ellipses denote the remaining terms<sup>4</sup>.

<sup>3</sup> The factor  $z^{1-s}$  was included in the r.h.s. of (4.17) and (4.19) to simplify the form of the recurrence relations.

<sup>4</sup> Equation (4.21) describes solutions only for  $h = (1 + n_h)/2$  where  $n_h \in 2\mathbb{Z}$ .

Substituting (4.20) and (4.21) into (4.1) and performing integration over the region of  $|1 - z| \ll 1$ , one can find the asymptotic behaviour of  $Q(u, \bar{u})$  at large  $u$ .

Let us consider the duality relation (4.4). Using the function  $Q(z, \bar{z})$  we evaluate (4.20) in the limit  $|z| \rightarrow 1$ . In this way, we obtain set of relations for the functions  $\beta_i(q, \bar{q})$  and  $\gamma_{m\bar{m}}(q, \bar{q})$ . The derivation is based on the following property

$$Q_a^{(1)}(1/z; -q) = \sum_{b=1}^N S_{ab} Q_b^{(1)}(z; q), \quad (4.22)$$

with  $\text{Im}(1/z) > 0$  and where the dependence on the integrals of motion was explicitly indicated. Here taking limit  $z \rightarrow 1$  in (4.17) and (4.18) and substituting them to (4.22) we are able to evaluate the  $S$ -matrix

$$S_{11} = e^{-i\pi(Ns-h-1)}, \quad S_{22} = e^{-i\pi(Ns+h-2)}, \quad S_{k,k+m} = (-1)^{k-3} \frac{(k-2s-1)_m}{m!} \quad (4.23)$$

with  $(x)_m \equiv \Gamma(x+m)/\Gamma(x)$ ,  $3 \leq k \leq N$  and  $0 \leq m \leq N-k$ . Similar relations hold in the anti-holomorphic sector,

$$\bar{S}_{11} = e^{i\pi(N\bar{s}-\bar{h}-1)}, \quad \bar{S}_{22} = e^{i\pi(N\bar{s}+\bar{h}-2)}, \quad \bar{S}_{k,k+m} = (-1)^{k-3} \frac{(k-2\bar{s}-1)_m}{m!}. \quad (4.24)$$

The  $S$ -matrix does not depend on  $z$  because the  $Q$ -functions on the both sides of relation (4.22) satisfy the same differential equation (4.2).

Now, substituting (4.20) and (4.22) into (4.4), we find

$$\begin{aligned} \beta_h(q, \bar{q}) &= e^{i\theta_N(q, \bar{q})} (-1)^{Nn_s+n_h} \beta_h(-q, -\bar{q}), \\ \gamma_{m\bar{m}}(q, \bar{q}) &= e^{i\theta_N(q, \bar{q})} \sum_{n, \bar{n} \geq 3}^N S_{nm} \gamma_{n\bar{n}}(-q, -\bar{q}) \bar{S}_{\bar{n}\bar{m}}. \end{aligned} \quad (4.25)$$

In this way, similarly to the energy, Eq. (4.15), which was calculated from the mixing matrix at  $z = 0$ , the eigenvalues of the quasimomentum,  $\theta_N(q, \bar{q})$ , can be calculated from the mixing matrix at  $z = 1$ , from the first relation (4.25). In the special case when  $q_{2k+1} = \bar{q}_{2k+1} = 0$  ( $k = 1, 2, \dots$ ), this means  $\beta_h(q, \bar{q}) = \beta_h(-q, -\bar{q})$ , the quasimomentum is equal to

$$e^{i\theta_N(q, \bar{q})} = (-1)^{Nn_s+n_h}. \quad (4.26)$$

### 4.3. Transition matrices

In the previous Sections we constructed the solutions  $Q(z, \bar{z})$  to (4.2) in the vicinity of  $z = 0$  and  $z = 1$ . Now, we glue these solutions inside

the region  $|1 - z| < 1$ ,  $|z| < 1$  and, then analytically continue the resulting expression for  $Q(z, \bar{z})$  into the whole complex  $z$ -plane by making use of the duality relation (4.4).

Firstly, we define the transition matrices  $\Omega(q)$  and  $\bar{\Omega}(\bar{q})$ :

$$Q_n^{(0)}(z) = \sum_{m=1}^N \Omega_{nm}(q) Q_m^{(1)}(z), \quad \bar{Q}_n^{(0)}(\bar{z}) = \sum_{m=1}^N \bar{\Omega}_{nm}(\bar{q}) \bar{Q}_m^{(1)}(\bar{z}). \quad (4.27)$$

which are uniquely fixed [17]. The resulting expressions for the matrices  $\Omega(q)$  and  $\bar{\Omega}(\bar{q})$  take the form of infinite series in  $q$  and  $\bar{q}$ , respectively. Substituting (4.27) into (4.9) and matching the result into (4.20), we find the following relation

$$C^{(1)}(q, \bar{q}) = [\Omega(q)]^T C^{(0)}(q, \bar{q}) \bar{\Omega}(\bar{q}). \quad (4.28)$$

The above matrix equation allows us to determine the matrices  $C^{(0)}$  and  $C^{(1)}$  and provides the quantization conditions for the integrals of motion,  $q_k$  and  $\bar{q}_k$  with  $k = 3, \dots, N$ . Therefore, we can evaluate the eigenvalues of the Baxter  $\mathbb{Q}$ -operator, Eq. (4.1). Formula (4.28) contains  $N^2$  equations with:

- $(N - 1)$   $\alpha$ -parameters inside the matrix  $C^{(0)}$ ,
- $2 + (N - 2)^2$  parameters  $\beta_{1,2}$  and  $\gamma_{m\bar{m}}$  inside the matrix  $C^{(1)}$ ,
- $(N - 2)$  integrals of motion  $q_3, \dots, q_N$  where  $\bar{q}_k = q_k^*$

Thus, we obtain  $(2N - 3)$  nontrivial consistency conditions.

The solutions to the quantization conditions (4.28) will be presented in detail in next Sections.

## 5. Properties of the $N$ -Reggeon states

In this Section we characterize the spectra of the conformal charges obtained by numerical calculations [17, 34]. Here, parametrization of the spectra is presented and the spectrum symmetries are shown. Moreover, descendent states are described.

### 5.1. Trajectories

Solving quantization conditions (4.28) we obtain continuous trajectories in the space of conformal charges. They are built of points,  $(q_2(\nu_h), \dots, q_N(\nu_h))$  which satisfy (4.28) and depend on a continuous real parameter  $\nu_h$  entering  $q_2$ , (2.35) and (2.27). In order to label the trajectories we introduce the set of the integers

$$\ell = \{\ell_1, \ell_2, \dots, \ell_{2(N-2)}\} \quad (5.1)$$

which parameterize one specified point on each trajectory for given  $h$ . Specific examples in the following sections will further clarify this point.

Next we calculate the observables along these trajectories, namely the energy (4.15) and the quasimomentum (4.25). The quasimomentum is constant (2.38) for all points situated on a given trajectory. The minimum of the energy, which means the maximal intercept, for almost all trajectories is located at  $\nu_h = 0$ . It turns out that the energy behaves around  $\nu_h = 0$  like

$$E_N(\nu_h; \ell^{\text{ground}}) = E_N^{\text{ground}} + \sigma_N \nu_h^2 + \mathcal{O}(\nu_h^2) \quad (5.2)$$

Thus, the ground state along its trajectory is gapless and the leading contribution to the scattering amplitude around  $\nu_h$  may be rewritten as a series in the strong coupling constant:

$$\mathcal{A}(s, t) \sim -is \sum_{N=2}^{\infty} (i\bar{\alpha}_s)^N \frac{s^{-\bar{\alpha}_s E_N^{\text{ground}}/4}}{(\bar{\alpha}_s \sigma_N \ln s)^{1/2}} \xi_{A,N}(t) \xi_{B,N}(t), \quad (5.3)$$

where  $\bar{\alpha}_s = \alpha_s N_c / \pi$  and  $\xi_{X,N}(t)$  are the impact factors corresponding to the overlap between the wave-functions of scattered particle with the wave-function of  $N$ -Reggeons, whereas  $\sigma_N$  measures the dispersion of the energy on the the trajectory around  $\nu_h = 0$ .

On the other hand, the energy along the trajectories grows with  $\nu_h$  and for  $|\nu_h| \rightarrow \infty$  and finally, we have  $E_N(\nu_h; \ell) \sim \ln \nu_h^2$ . These parts of the trajectory give the lowest contribution to the scattering amplitude.

## 5.2. Symmetries

The spectrum of quantized charges  $q_2, \dots, q_N$  is degenerate. This degeneration is caused by two symmetries:

$$q_k \leftrightarrow (-1)^k q_k \quad (5.4)$$

which comes from invariance of the Hamiltonian under mirror permutations of particles, (2.36), and

$$q_k \leftrightarrow \bar{q}_k \quad (5.5)$$

which is connected with the symmetry under interchange of the  $z$ - and  $\bar{z}$ -sectors. Therefore, the four points,  $\{q_k\}$ ,  $\{(-1)^k q_k\}$ ,  $\{q_k^*\}$  and  $\{(-1)^k q_k^*\}$  with  $k = 2, \dots, N$ , are related and all of them satisfy the quantization conditions (4.28) and have the same energy.



### 5.3. Descendent states

Let us first discuss the spectrum along the trajectories with the highest conformal charge  $q_N$  equal zero for arbitrary  $\nu_h \in \mathbb{R}$ . It turns out [35, 36, 37, 17] that the wave-functions of these states are built of  $(N - 1)$ -particle states. Moreover, their energies [38] are also equal to the energy of the ancestor  $(N - 1)$ -particle states:

$$E_N(q_2, q_3, \dots, q_N = 0) = E_{N-1}(q_2, q_3, \dots, q_{N-1}). \quad (5.6)$$

Thus, we call them the descendent states of the  $(N - 1)$ -particle states.

Generally, for odd  $N$ , the descendent state  $\Psi_N^{(q_N=0)}$  with the minimal energy  $E_N(q_N = 0) = 0$  has for  $q_2 = 0$ , *i.e.* for  $h = 0, 1$ , the remaining integrals of motion  $q_3 = \dots = q_N = 0$  as well. For  $h = 1 + i\nu_h$ , *i.e.*  $q_2 \neq 0$ , the odd conformal charges  $q_{2k+1} = 0$  with  $k = 1, \dots, (N - 1)/2$  while the even ones  $q_{2k} \neq 0$  and depend on  $\nu_h$ .

On the other hand, for even  $N$ , the eigenstate with the minimal energy  $\Psi_N^{(q_N=0)}$  is the descendent state of the  $(N - 1)$ -particle state which has minimal energy with  $q_{N-1} \neq 0$ . Thus,  $E_N^{min}(q_N = 0) = E_{N-1}^{min}(q_{N-1} \neq 0) > 0$ .

Studying more exactly this problem one can obtain [35, 17] a relation between the quasimomentum  $\theta_N$  of the descendent state and the ancestor one  $\theta_{N-1}$ , which takes the following form

$$e^{i\theta_N} \Big|_{q_N=0} = -e^{i\theta_{N-1}} = (-1)^{N+1}. \quad (5.7)$$

Additionally, one can define a linear operator  $\Delta$  [35, 17] that maps the subspace  $V_{N-1}^{(q_N=0)}$  of the  $(N - 1)$ -particle ancestor eigenstates with the quasimomentum  $\theta_{N-1} = \pi N$  into the  $N$ -particle descendent states with  $q_N = 0$  and  $\theta_N = \pi(N + 1)$  as

$$\Delta : V_{N-1}^{(\theta_{N-1}=\pi N)} \rightarrow V_N^{(\theta_N=\pi(N+1))}. \quad (5.8)$$

It turns out that this operator is nilpotent for the eigenstates which form trajectories [35], *i.e.*  $\Delta^2\Psi = 0$ . Thus, the descendent-state trajectory can not be ancestor one for  $(N + 1)$ -particle states. However, it is possible to build a single state [17] with  $q_2 = q_3 = \dots = q_N = 0$ , *i.e.* for only one point  $\nu_h = 0$ , that has  $E_N = 0$  and the eigenvalue of Baxter  $Q$ -operator defined as

$$Q_N^{q=0}(u, \bar{u}) \sim \frac{u - \bar{u}}{\bar{u}^N}, \quad (5.9)$$

where a normalization factor was omitted.

Additional examples of the descendent states will be described later in the next sections.

## 6. Quantum numbers of the $N = 4$ states

In this Section we present the spectrum for four Reggeons calculated by making use of  $Q$ -Baxter method. To this end we resum solutions (4.8) and (4.18) numerically, and using them we solve the quantization conditions (4.28). Earlier, some results for  $N = 4$  were only presented in [17] and some numerical results in Ref. [18]. Here we show much more data and we present more detailed analysis of this spectrum. i.e. resemblant and winding spectra of  $q_3, q_4$  and corrections to the WKB approximation for  $N = 4$ .

For four Reggeons the spectrum of the conformal charges is much more complicated than in the three-Reggeon case [20]. Indeed, we have here the space of three conformal charges  $(q_2, q_3, q_4)$ . Thus, apart from the lattice structure in  $q_4^{1/4}$  we have also respective lattice structures in  $q_3$ -space. Here we consider the case for  $n_h = 0$  so that  $h = \frac{1}{2} + i\nu_h$ . This spectrum includes the ground states. For clarity we split these spectra into several parts. We perform this separation by considering spectra with different quasimomenta  $\theta_4(q, \bar{q})$  as well as a different quantum number  $\ell_3$ , which will be defined in the solution (6.2)–(6.3) of two quantization conditions (4.28) for  $N = 4$  from Ref. [15].

From the first quantization condition of WKB approximation [15] one can get the WKB approximation of the charge  $q_4$  as

$$q_4^{1/4} = \frac{\Gamma^2(3/4)}{4\sqrt{\pi}} \left[ \frac{1}{\sqrt{2}}\ell_1 + \frac{i}{\sqrt{2}}\ell_2 \right] \quad (6.1)$$

and the quasimomentum is equal to

$$\theta_4 = -\frac{\pi}{2}\ell = \frac{\pi}{2}(\ell_2 + \ell_3 - \ell_1) \pmod{2\pi}, \quad (6.2)$$

where  $\ell_1, \ell_2$  and  $\ell_3$  are even for even  $\ell$  and odd for odd  $\ell$ . Thus, we have two kinds of lattices: with  $\theta_4 = 0, \pi$  and with  $\theta_4 = \pm\pi/2$ . They are presented in Fig. 1. In these pictures gray lines show the WKB lattice (6.1) with vertices at  $\ell_1, \ell_2 \in \mathbb{Z}$ . To find the leading approximation for the charge  $q_3$ , we apply the second relation of WKB approximation [15] gives

$$\text{Im} \frac{q_3}{q_4^{1/2}} = (\ell_1 - \ell_2 - \ell) = \ell_3. \quad (6.3)$$

Notice that the system (6.1) and (6.3) is underdetermined and it does not fix the charge  $q_3$  completely [15].

It turns out that after choosing one value of  $\theta_4$ , the lattice in  $q_4^{1/4}$ -space is still spuriously degenerated<sup>5</sup> and this degeneration also corresponds to

<sup>5</sup> degeneration in the leading order of the WKB approximation

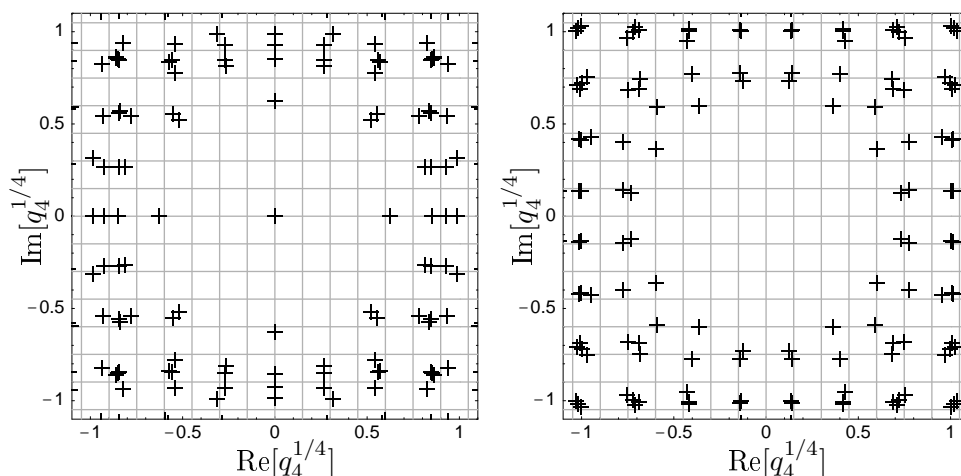


Figure 1. The spectrum of the integrals of motion  $q_4$  for  $N = 4$  and the total spin  $h = 1/2$ . The left and right panels correspond to the eigenstates with different quasimomenta  $e^{i\theta_4} = \pm 1$  and  $\pm i$ , respectively.

different lattices in  $q_3^{1/2}$ . The parameter  $\ell_3$  which is defined in (6.3) will be used to distinguish these different lattices.

### 6.1. Descendent states for $N = 4$

One can notice that for  $N = 4$  and  $n_h = 0$  we have the descendent states. They appear in sector with the quasimomentum  $\theta_4 = \pi$ , which agrees with (5.7). The wave-functions of the descendent states are built of three-particle eigenstates with  $\theta_3 = 0$ . Additionally, the spectrum of  $q_3$  for these three-Reggeon states and the descendent state for  $N = 4$  is the same and it is depicted in Fig. 2 on the left panel. Moreover, the energy of these descendent state and the corresponding three-Reggeon states are also the same (5.6).

### 6.2. Lattice structure for $q_3 = 0$

Let us consider the spectrum with  $q_4 \neq 0$  and  $q_3 = 0$ , see the right panel of Fig 2. In this case the quasimomentum  $\theta_4 = 0$  and the lattice structure include vertices that correspond to the ground state.

Similarly to the  $N = 3$  case [20] we have in the  $q_4^{1/4}$ -space a lattice with a square-like structure described by (6.1). In this case even numbers  $\ell_1$  and  $\ell_2$  satisfy  $\ell_1 + \ell_2 \in 4\mathbb{Z}$ . Thus, we have the WKB formula

$$[q_4^{\text{WKB}}(\ell_1, \ell_2)]^{1/4} = \Delta_{N=4} \cdot \left( \frac{\ell_1}{2\sqrt{2}} + i \frac{\ell_2}{2\sqrt{2}} \right), \quad (6.4)$$

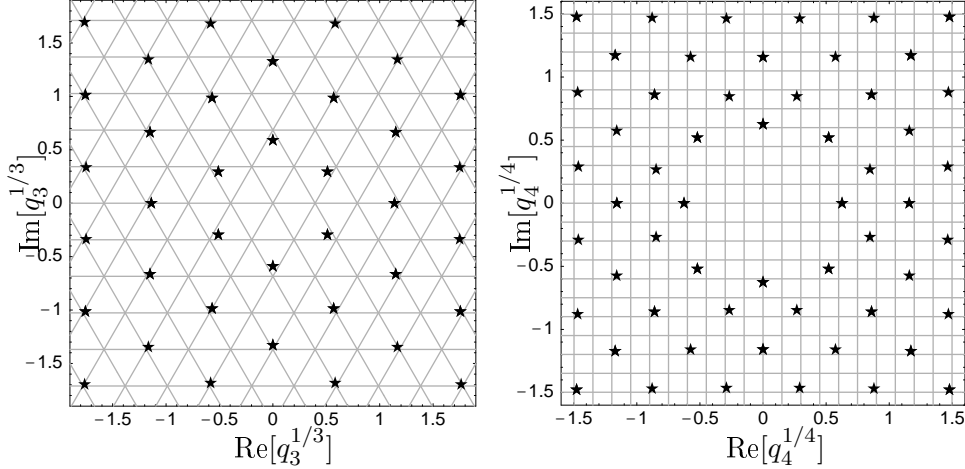


Figure 2. The spectra of the conformal charges for  $N = 4$  and comparison to the WKB expansion. On the left panel, the spectrum of  $q_3$  with  $q_4 = 0$  corresponding to the descendent states with  $\theta_4 = \pi$ . On the right panel, the spectrum of  $q_4$  for  $h = 1/2$  and  $q_3 = 0$  with  $\theta_4 = 0$ . The WKB lattices are denoted by the gray lines.

where the vertices are placed outside a disk around the origin of the radius

$$\Delta_4 = \left[ \frac{4^{3/4}}{\pi} \int_{-1}^1 \frac{dx}{\sqrt{1-x^4}} \right]^{-1} = \frac{\Gamma^2(3/4)}{2\sqrt{\pi}} = 0.423606\dots \quad (6.5)$$

As before, the leading-order WKB formula (6.4) is valid only for  $|q_4^{1/4}| \gg |q_2^{1/2}|$ .

The energy is lower for points which are nearer to the origin. Similarly to the  $N = 3$  case, the spectrum is also built of trajectories which extend in the  $(\nu_h, q_3, q_4)$ -space. Namely, each point on the  $q_4^{1/4}$ -lattice belongs to one specific trajectory parameterized by the set of integers  $\{\ell_1, \ell_2, \dots\}$ .

The ground state for  $N = 4$  is situated on a trajectory with  $(\ell_1, \ell_2) = (4, 0)$ . We find that for this trajectory  $q_3 = \text{Im } q_4 = 0$ , whereas  $\text{Re}[q_4]$  and  $E_4$  vary with  $\nu_h$  as we show in Figure 3. An accumulation of the energy levels in the vicinity of  $\nu_h = 0$  is described by Eq. (5.2) with the dispersion parameter  $\sigma_4 = 5.272$ .

On the  $q_4^{1/4}$ -plane the ground state is represented by four points with the coordinates  $(\ell_1, \ell_2) = (\pm 4, 0)$  and  $(0, \pm 4)$ . Due to a residual symmetry  $q_4^{1/4} \leftrightarrow \exp(ik\pi/2)q_4^{1/4}$ , they describe a single eigenstate with

$$q_3^{\text{ground}} = 0, \quad q_4^{\text{ground}} = 0.153589\dots, \quad E_4^{\text{ground}} = -2.696640\dots \quad (6.6)$$

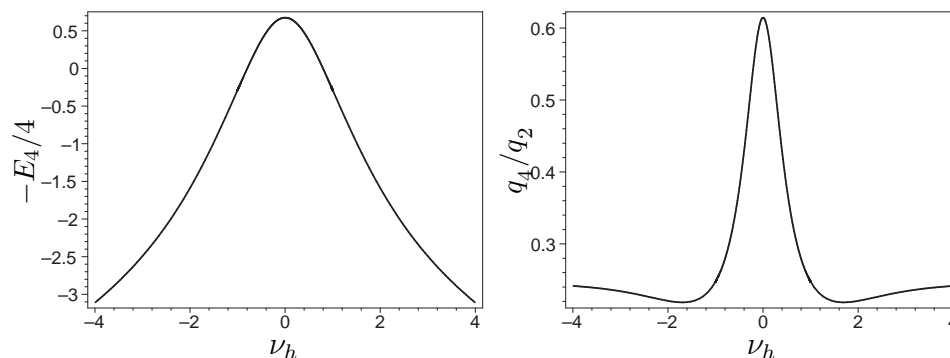


Figure 3. The dependence of the energy,  $-E_4/4$ , and the quantum number,  $q_4/q_2$ , with  $q_2 = 1/4 + \nu_h^2$ , on the total spin  $h = 1/2 + i\nu_h$  along the ground state trajectory for  $N = 4$ .

with  $h = 1/2$ . It has the quasimomentum  $\theta_4 = 0$  and, in contrast to the  $N = 3$  case, it is unique.

$(\ell_1/2, \ell_2/2)$	$(q_4^{\text{exact}})^{1/4}$	$(q_4^{\text{WKB}})^{1/4}$	$-E_4/4$
(2, 0)	0.626	0.599	0.6742
(2, 2)	$0.520 + 0.520 i$	$0.599 + 0.599 i$	-1.3783
(3, 1)	$0.847 + 0.268 i$	$0.899 + 0.299 i$	-1.7919
(4, 0)	1.158	1.198	-2.8356
(3, 3)	$0.860 + 0.860 i$	$0.899 + 0.899 i$	-3.1410
(4, 2)	$1.159 + 0.574 i$	$1.198 + 0.599 i$	-3.3487

Table 1. Comparison of the exact spectrum of  $q_4^{1/4}$  at  $q_3 = 0$  and  $h = 1/2$  with the approximate WKB expression 6.4. The last column shows the exact energy  $E_4$ .

The comparison of (6.4) with the exact results for  $q_4$  at  $h = 1/2$  is shown in Figure 2 and Table 1. One can see that the WKB formula (6.4) describes the spectrum with a good accuracy.

### 6.3. Resemblant lattices with $\ell_3 = 0$

In the previous Section we introduced the parameter  $\ell_3$  which helps us to distinguish different lattices. This parameter takes even values for  $\theta_4 = 0, \pi$  and odd ones for  $\theta_4 = \pm\pi/2$ . Let us take  $\ell_3 = 0$ . It turns out that in this case the spectrum lattice in the  $q_3^{1/2}$ -space is similar to the corresponding lattice in the  $q_4^{1/4}$ -space, *i.e.* considering only the leading order of the WKB

approximation the  $q_3^{1/2}$ -lattice in comparison to the  $q_4^{1/4}$ -lattice is rescaled by some real number. An example of such a lattice for  $\theta_4 = 0$  is shown in Figure 4. One can notice that the non-leading corrections to the WKB approximation cause the bending of the lattice structure in Fig. 4: for  $q_4^{1/4}$  concave whereas for  $q_3^{1/2}$  convex. Moreover, we can see the  $q_4^{1/4}$ -lattice as well as  $q_3^{1/2}$ -one have a similar structure to the lattice with  $q_3 = 0$  presented in Fig. 2. These lattices also do not have the vertices inside the disk at the origin  $q_3 = q_4 = 0$ .

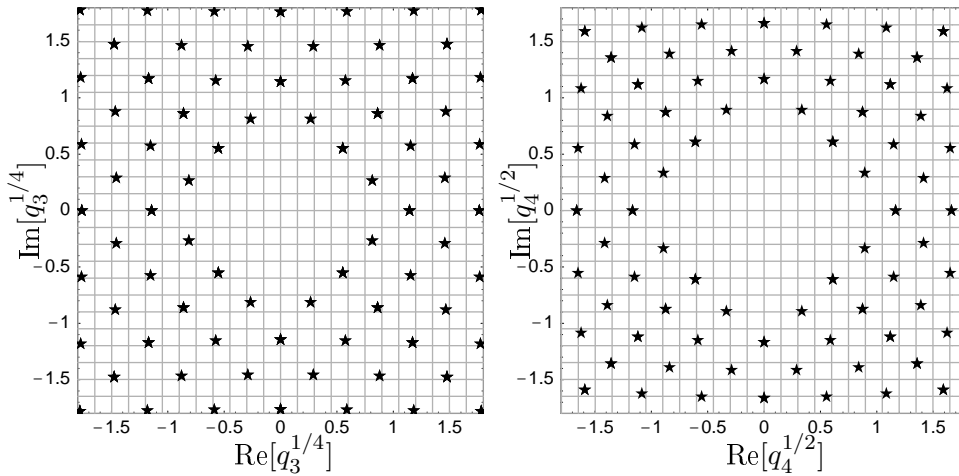


Figure 4. The spectra of the conformal charges for  $N = 4$  with  $\theta_4 = 0$ ,  $\ell_3 = 0$  and  $\ell_4 = 1$ . On the left panel the spectrum of  $q_4^{1/4}$ , while on the right panel the spectrum of  $q_3^{1/2}$

Substituting

$$q_3^{1/2} = r_3 e^{i\phi_3} \quad \text{and} \quad q_4^{1/4} = r_4 e^{i\phi_4} \quad (6.7)$$

into (6.3) we obtain a condition for the leading order of the WKB approximation

$$\ell_3 = \left( \frac{r_3}{r_4} \right)^2 \sin(2(\phi_3 - \phi_4)). \quad (6.8)$$

Thus, for  $\ell_3 = 0$  and for a scale  $\lambda = r_3/r_4 > 0$  we have  $\phi_3 = \phi_4$ . This means that the vertices on the  $q_3^{1/2}$ -lattice have the same angular coordinates as those from the  $q_4^{1/4}$ -lattice. Looking at the numerical results in Figure 4 we notice that the missing quantization condition for  $\ell_3 = 0$  in the leading

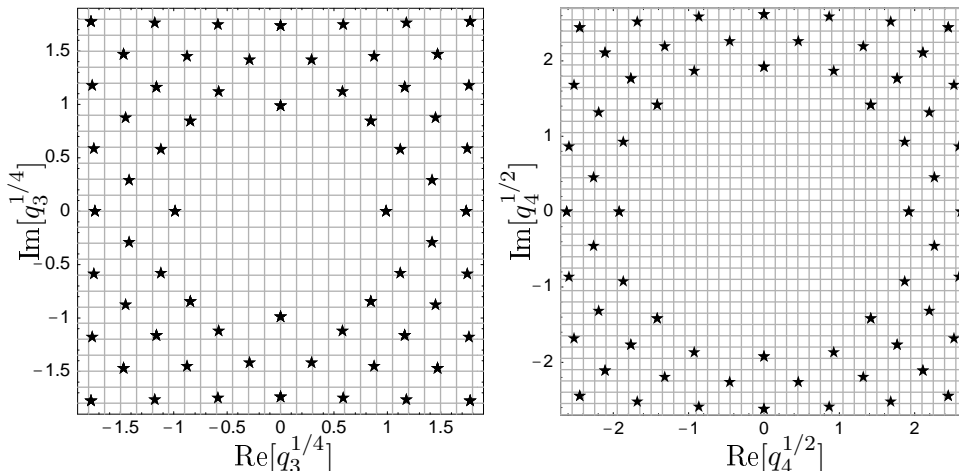


Figure 5. The spectra of the conformal charges for  $N = 4$  with  $\theta_4 = 0$ ,  $\ell_3 = 0$  and  $\ell_4 = 2$ . On the left panel the spectrum of  $q_4^{1/4}$ , while on the right panel the spectrum of  $q_3^{1/2}$

WKB order should have a form similar to

$$\left| \frac{q_3}{q_4^{1/2}} \right| = \lambda_{\ell_4}^2, \tag{6.9}$$

where  $\lambda_{\ell_4} = r_3/r_4 \in \mathbb{R}$  is a constant scale for a given lattice  $\ell_4$ .

It turns out that for a specified quasimomentum we have an infinite number of such lattices. They differ from each other by a given scale  $\lambda_{\ell_4}$ . For example for  $\theta_4 = 0$  we have another lattice, shown in Fig 5. Its scale  $\lambda_2$  differs from the scale  $\lambda_1$  of the lattice from Fig. 4. The resemblant  $q_4^{1/4}$ -lattices for  $\theta_4 = 0$  are described by (6.1) with the integer parameters  $\ell_1$  and  $\ell_2$  satisfying  $\ell_1 + \ell_2 \in 4\mathbb{Z}$ .

The similar lattices also exist in the sector with the quasimomentum  $\theta_4 = \pi$ . Some of them are presented in Figures 6 and 7. For  $\theta_4 = \pi$  the resemblant  $q_4^{1/4}$ -lattices are also described by (6.1) but the integer parameters  $\ell_1$  and  $\ell_2$  satisfy  $\ell_1 + \ell_2 \in 4\mathbb{Z} + 2$ .

#### 6.4. Winding lattices with $\ell_3 \neq 0$

In the case with  $\ell_3 \neq 0$  we have much more complicated situation than for  $\ell_3 = 0$ . According to (6.8) the angles  $\phi_3$  and  $\phi_4$  defined in (6.7) are no more equal. Moreover, they start to depend on the scale  $\lambda = r_3/r_4$ .

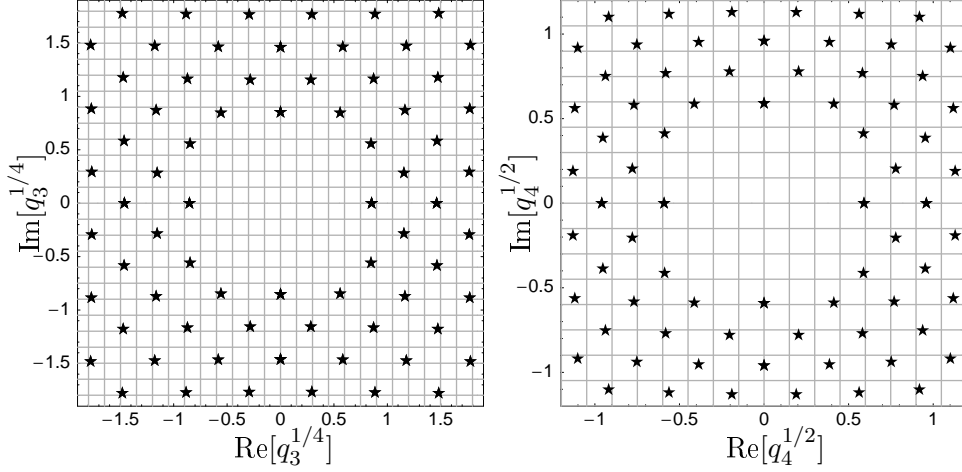


Figure 6. The spectra of the conformal charges for  $N = 4$  with  $\theta_4 = \pi$ ,  $\ell_3 = 0$  and  $\ell_4 = 1$ . On the left panel the spectrum of  $q_4^{1/4}$ , while on the right panel the spectrum of  $q_3^{1/2}$

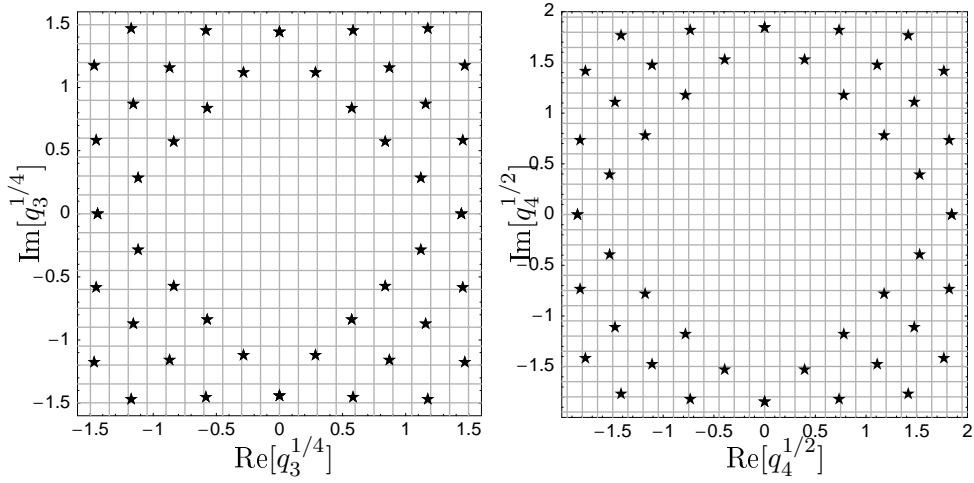


Figure 7. The spectra of the conformal charges for  $N = 4$  with  $\theta_4 = \pi$ ,  $\ell_3 = 0$  and  $\ell_4 = 2$ . On the left panel the spectrum of  $q_4^{1/4}$ , while on the right panel the spectrum of  $q_3^{1/2}$

An example of such a lattice, with  $\ell_3 = 1$  and  $\theta_4 = -\pi/2$  we show in Figure 8. For this case, the  $q_4^{1/4}$ -lattice is defined by (6.1) with  $\ell_1$  and  $\ell_2$  odd integer numbers satisfying  $\ell_1 + \ell_2 \in 4\mathbb{Z}$ . In Figure 8, in order to present the correspondence between the  $q_3^{1/2}$ - and  $q_4^{1/4}$ -lattice, we depict only some vertices of the lattice which extends in the whole plane of the conformal



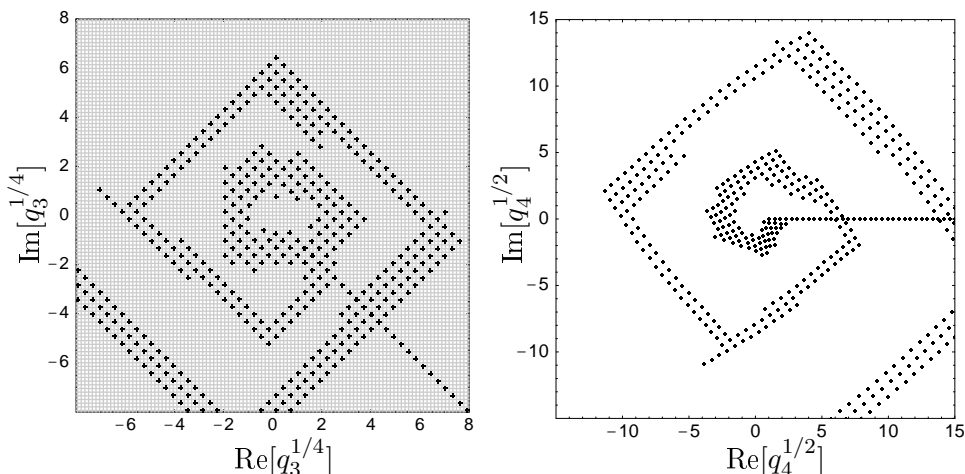


Figure 8. The winding spectrum of the conformal charges for  $N = 4$  and  $h = 1/2$  with  $\theta_4 = -\pi/2$  and  $\ell_3 = 1$ . On the left panel the spectrum of  $q_4^{1/4}$ , while on the right panel the spectrum of  $q_3^{1/2}$

charges except the place nearby the origin  $q_4 = q_3 = 0$ . As we can see the  $q_3^{1/2}$ -lattice is still a square-like one but it winds around the origin  $q_3^{1/2} = 0$ . Looking at Figure 8, let us start from  $\phi_3 = 0$  and  $\phi_4 = -\pi/4$  where  $\phi_3$  and  $\phi_4$  are defined in (6.7). Thus, the difference  $\phi_3 - \phi_4 = \pi/4$  so that our scale at the beginning is  $\lambda = \sqrt{2}$ . In this region the vertices of the  $q_3^{1/2}$ -lattice are in the nearest place to the origin. When we go clockwise around the origin of the lattices by decreasing  $\phi_4$ , we notice that  $\phi_3$  also decreases but much slower. Thus, according to (6.8) the difference  $\phi_3 - \phi_4$  changes. Moreover, due to (6.8), the scale  $\lambda$  also continuously rises. Therefore, the  $q_3^{1/2}$ -lattice winds in a different way than the  $q_4^{1/4}$ -lattice. After one revolution the vertices of the  $q_4^{1/4}$ -lattices are at similar places as those with  $\phi_4$  decreased by  $2\pi$ . This provides additional spurious degeneration in  $q_4^{1/4}$ . However, after revolution by the angle  $2\pi$ , the vertices in  $q_3^{1/2}$ -space have completely different conformal charges  $q_3$ . The spurious degeneration in the  $q_3^{1/2}$ -lattice does not appear.

We have to add that we obtain the second symmetric structure when we go in the opposite direction, *i.e.* anti-clockwise. Moreover, the winding lattice, like all other lattices, extends to infinity on the  $q_3^{1/2}$ - and  $q_4^{1/4}$ -plane and does not have vertices in vicinity of the origin,  $q_3 = q_4 = 0$ . However, the radii of these empty spaces grow with  $\phi_{3,4}$ .

Additionally, due to symmetry of the spectrum (5.5) we have a twin

lattice with  $q_k \rightarrow q_k^*$ . Furthermore, the second symmetry (5.4) produces another lattice rotated in the  $q_3^{1/2}$ -space by an angle  $\pi/2$ . Notice that this symmetry (5.4) exchanges quasimomentum  $\theta_4 \leftrightarrow 2\pi - \theta_4 \pmod{2\pi}$ . Thus, the spectrum for  $\theta_4 = \pi/2$  is congruent with the spectrum of  $\theta_4 = -\pi/2$  but it is rotated in the  $q_3^{1/2}$ -space by  $\pi/2$ .

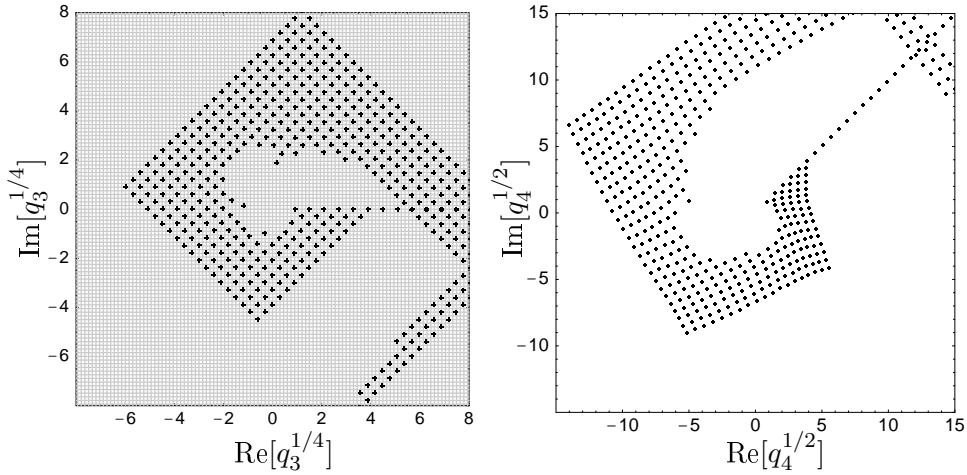


Figure 9. The winding spectrum of the conformal charges for  $N = 4$  with  $h = 1/2$ ,  $\theta_4 = 0$  and  $\ell_3 = 2$ . On the left panel the spectrum of  $q_4^{1/4}$  while on the right panel the spectrum of  $q_3^{1/2}$

As we said before for  $\theta_4 \pm \pi/2$  we have winding spectra with odd  $\ell_3$ . Similarly, for even  $\ell_3 \neq 0$  we have winding spectra with  $\theta_4 = 0, \pi$ , thus, the lattice with the lowest non-zero  $\ell_3$  corresponds to  $|\ell_3| = 2$ . We present some points of this spectrum in Fig. 9, for which  $\ell_1, \ell_2$  in (6.1) are even and  $\ell_1 + \ell_2 \in 4\mathbb{Z} + 2$ . In this case we start with  $\phi_3 = \pi/4$  and  $\phi_4 = 0$  which implies the beginning scale  $\lambda = \sqrt{2}$ . The spectra wind as in the previous case.

Similarly, for  $\theta_4 = \pi$  we have also spectrum with the lowest  $|\ell_3| = 2$ . It is defined by (6.1) with  $\ell_1, \ell_2$  even and  $\ell_1 + \ell_2 \in 4\mathbb{Z}$ . In this case the angles  $\phi_3 = 0$  and  $\phi_4 = -\pi/4$  so we also have the beginning scale  $\lambda = \sqrt{2}$ , as depicted in Figure 10. In order to describe the winding spectra better we may introduce an integer parameter  $\ell_4$  which helps us to number the overlapping winding planes of the spectra and name spuriously-degenerated vertices in the  $q_4^{1/4}$ -plane.

To sum up, even for a given quasimomentum we have many lattices which overlap, so that vertices of the lattices, especially in  $q_3^{1/2}$ -space, make an impression of being randomly distributed. However, as we have shown above,

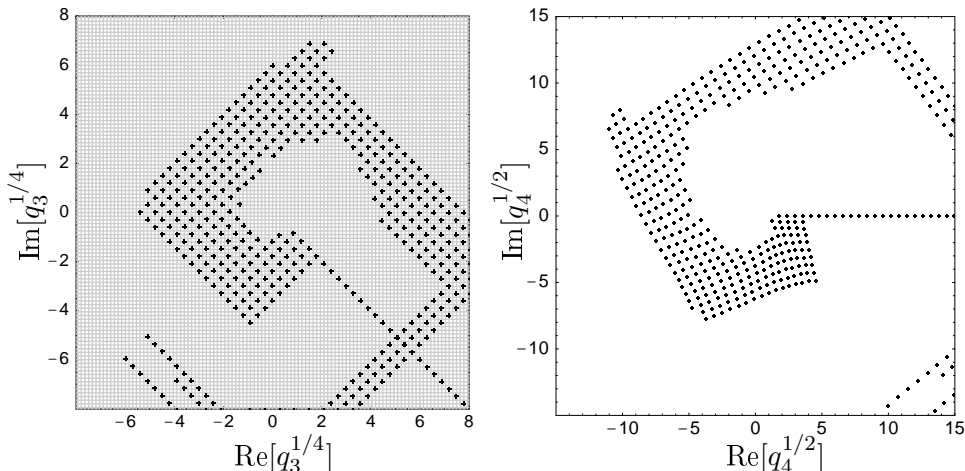


Figure 10. The winding spectrum of the conformal charges for  $N = 4$  with  $h = 1/2$ ,  $\theta_4 = \pi$  and  $\ell_3 = 2$ . On the left panel the spectrum of  $q_4^{1/4}$  while on the right panel the spectrum of  $q_3^{1/2}$

those spectra may be distinguished and finally described by (6.1) and (6.3). Still, there is a lack of one nontrivial WKB condition which would uniquely explain the structure of the resemblant and winding lattices.

### 6.5. Corrections to WKB

Let us consider the spectrum of the conformal charge  $q_4$  for  $N = 4$  with  $q_3 = 0$  and  $h = \frac{1+n_h}{2}$ . It turns out that for  $n_h \neq 0$  it has similar square-like lattice structure like that with  $n_h = 0$ , see Fig. 2 on the right panel. Similarly to the case with three reggeized gluons [20] we have evaluated the conformal charges  $q_4$  with even  $n_h$  with high precision. We have done it separately for  $q_4$  with  $\text{Im}[q_4] = 0$  and  $\text{Re}[q_4] = 0$ . Next, we have fitted coefficient expansion of the WKB series,  $a_k^{(r)}$  and  $a_k^{(i)}$ , respectively.

In [15] the series formula for  $q_4^{1/4}$  looks as follows

$$q_4^{1/4} = \frac{\pi^{3/2}}{2\Gamma^2(1/4)} \mathcal{Q}(\mathbf{n}) \left[ 1 + \frac{b}{|\mathcal{Q}(\mathbf{n})|^2} + \sum_{k=2}^{\infty} a_k \left( \frac{b}{|\mathcal{Q}(\mathbf{n})|^2} \right)^k \right], \quad (6.10)$$

where

$$\mathcal{Q}(\mathbf{n}) = \sum_{k=1}^4 n_k e^{i\pi(2k-1)/4} = \left( \frac{\ell_1}{\sqrt{2}} + i \frac{\ell_2}{\sqrt{2}} \right) \quad (6.11)$$

and  $\ell_1, \ell_2, \mathbf{n} = \{n_1, \dots, n_N\}$  are integer.

$n_h$	coef.	$k = 2$	$k = 3$	$k = 4$	$k = 5$
0	$a_k^{(r)}$	2.9910566246	-24.021689	91.591	645.5
	$a_k^{(i)}$	-4.9910566246	28.021689	-148.830	1656.7
	$a_k^{(r)} + a_k^{(i)}$	-2.0000000000	4.000000	-57.239	2302.2
2	$a_k^{(r)}$	-1.3991056625	4.674008	-4.516	-95.7
	$a_k^{(i)}$	-0.6008943375	-0.674008	20.388	-200.8
	$a_k^{(r)} + a_k^{(i)}$	-2.0000000000	4.000000	15.872	-296.5
4	$a_k^{(r)}$	-1.351212983	3.462323	-11.322	43.164
	$a_k^{(i)}$	-0.648787017	0.537677	-0.096	0.611
	$a_k^{(r)} + a_k^{(i)}$	-2.0000000000	4.000000	-11.418	43.775
6	$a_k^{(r)}$	-0.8882504145	1.883461	-5.4248	18.081
	$a_k^{(i)}$	-1.1117495855	2.116539	-4.8117	12.091
	$a_k^{(r)} + a_k^{(i)}$	-2.0000000000	4.000000	-10.2365	30.172
8	$a_k^{(r)}$	-0.6326570719	1.197694	-2.94579	8.3372
	$a_k^{(i)}$	-1.3673429281	2.802305	-5.96129	12.1238
	$a_k^{(r)} + a_k^{(i)}$	-2.0000000000	4.000000	-8.90708	20.4610

Table 2. The fitted coefficient to the series formula of  $q_4^{1/4}$  (6.10) with  $n_h = 0, 2, 4, 6$  and 8

Here for  $N = 4$ , similarly to the  $N = 3$  case in Ref. [20], we have a different expansion parameter  $b/|\mathcal{Q}(\mathbf{n})|^2$  and in this case the parameter

$$b = \frac{4}{\pi} \left( q_2^* - \frac{5}{4} \right) \quad (6.12)$$

is decreased by  $5/4$ . The expansion coefficients of the series (6.10) are shown in Table 2. Similarly to [15] the coefficients  $a_0 = 1$  and  $a_1 = 1$ . The remaining coefficients depend on  $n_h$ . Moreover, the coefficients  $a_k$  with  $k > 1$  are different for real  $q_4^{1/4}$  and for imaginary  $q_4^{1/4}$  but one may notice that for  $k = 1, 2$  the sum  $a_k^{(r)} + a_k^{(i)} \in \mathbb{Z}$  and does not depend on  $n_h$ . Thus, to describe the quantized values of  $q_4^{1/4}$  more generally one has to use both sets of the coefficients,  $a_k^{(r)}$  and  $a_k^{(i)}$ , or perform the expansion with two small independent parameters, *i.e.*  $q_2^*/|\mathcal{Q}(\mathbf{n})|^2$  and  $1/|\mathcal{Q}(\mathbf{n})|^2$ .

Using the series (6.10) with (6.12) and coefficients from Table 2 gives good approximation of the conformal charges  $q_4$  with  $q_3 = 0$ . However, in order to have a better precision one has to introduce an additional expansion parameter.

## 7. Summary and Conclusions

In this paper we discussed four Reggeon states which appear in scattering amplitude of strongly interacting particles in high energy Regge limit of QCD (2.1), *i.e.* in Generalized Leading Logarithm Approximation (GLLA) [9, 10, 39]. Due to the colour factor description of  $N$ -Reggeon system is a complicated task especially for  $N > 3$ . To this end multi-colour limit is performed. In this limit the Reggeon Hamiltonian separates into two one-dimensional equations and as a result the multi-Reggeon system get completely solvable. However, in order to solve it one has to use advanced integrable-model methods.

In the multi-colour limit the equation for the  $N$ -Reggeon wave-function takes a form of Schrödinger equation (2.10) for the non-compact XXX Heisenberg magnet model of  $SL(2, \mathbb{C})$  spins  $s$  [40, 33, 41]. Its Hamiltonian describes the nearest neighbour interaction of the Reggeons [42, 43] propagating in the two-dimensional transverse-coordinates space (2.6). The system has a hidden cyclic and mirror permutation symmetry (2.36). It also possesses the set of the  $(N - 1)$  of integrals of motion, which are eigenvalues of conformal charges [27],  $\hat{q}_k$  and  $\tilde{q}_k$ , (2.33)–(2.34). Therefore, the operators of conformal charges commute with each other and with the Hamiltonian and they possess a common set of the eigenstates.

To solve the Reggeon problem for more than three particles one uses the more sophisticated technique, *i.e.* the Baxter  $Q$ -operator method [27]. It relies on the existence of the operator  $\mathbb{Q}(u, \bar{u})$  depending on the pair of complex spectral parameters  $u$  and  $\bar{u}$ . The Baxter  $Q$ -operator has to commute with itself (3.1) and with the conformal charges (3.2). It also has to satisfy the Baxter equations (3.3)–(3.4). Furthermore, the  $Q$ -operator has well defined analytical properties, *i.e.* known pole structure (3.12) and asymptotic behaviour at infinity (3.14). The above conditions fix the  $Q$ -operator uniquely and allow to quantize the integrals  $q_k$ . It turns out [27] that the Reggeon Hamiltonian can be rewritten in terms of Baxter  $Q$ -operator (3.15). Therefore, combining together the solutions of the Baxter equations and the conditions for  $q_k$  with the Schrödinger equation, we can calculate the energy spectrum (3.24). Moreover, we are able to determine the quasimomentum of the eigenstates (3.20), *i.e.* the observable which defines the properties of the state with respect to the cyclic permutation symmetry (2.36).

In order to obtain the exact values of  $q_k$  we have used the method [15, 17] which consists in rewriting the Baxter equations and the other conditions for  $Q$ -operator eigenvalues as the  $N$ -order differential equation (4.2). Solving this equation one obtains the conditions for quantized  $q_k$  (4.28) and the formulae for the energy (4.15) and the quasimomentum (4.25).

In the case with  $N = 4$  particles we have constructed the spectrum for

$n_h = 0$  depicting complicated interplay between the conformal charges:  $q_3$  and  $q_4$ . Such a complete analysis has been performed here for the first time. Earlier, for  $N = 4$  full spectrum of  $q_4$  was shown in Ref. [17] (however the corresponding  $q_3$  spectrum was not discussed) and some values of  $q_4$  were found in Ref. [19]. The spectrum of  $q_4^{1/4}$  has a structure of square-like lattice (6.4), Fig. 1. In this case the spectrum of  $q_3$  is more complicated. It turns out that it has a few possible forms. Firstly, there are simple states with  $q_3 = 0$ , Fig. 2. Moreover, we have found the  $q_3^{1/2}$ -lattices whose distribution of vertices is similar to the distribution of vertices of  $q_4^{1/4}$ -lattice. We have called these structures as resemblant lattices, Figs. 4-7. Secondly we have demonstrated the existence of  $q_3^{1/2}$ -lattices that may be called winding lattices. They wind around the origin and in course of this winding the distance between vertices increases and also the lattice goes away from the origin, Figs. 8-10. The WKB approximation does not describe these structures (6.3) exactly because one quantization condition is missing. Finally, we have also considered the descendent states with  $q_4 = 0$ , Fig. 2. They have quasimomentum  $\theta_4 = \pi$  and the structure of their  $q_3^{1/3}$ -lattices is the same as for  $q_3^{1/3}$ -lattices in the three-Reggeon case with  $\theta_4 = 0$  [21, 20]. For the  $N = 4$  Reggeon states with  $q_3 = 0$  we have calculated corrections to the WKB approximation (6.10), Table 2. Similarly to the  $N = 3$  case [20] they come from the fact of using only one expansion parameter  $\eta$  for two different conformal charges,  $q_4$  and  $q_2$ . One has to notice that these corrections are subleading in comparison to the WKB limit [15].

The  $Q$ -Baxter method is complicated. However, it allows us to solve the reggeized gluon state problem for more than  $N = 3$  particles. The above calculations are of interest not only for perturbative QCD but also to statistical physics as the  $SL(2, \mathbb{C})$  non-compact XXX Heisenberg spin magnet model [40, 33, 41].

In order to find the full scattering amplitude one has to calculate the impact factors, *i.e.* overlaps between the Reggeon wave function and the wave functions of the scattered particles. These impact factors strongly depend on the scattered system and they are hard to calculate due to a large number of integrations. Thus, this work can be a first step in computing of contribution of the four-Reggeon state to the hadron scattering amplitude.

### Acknowledgements

I would like to warmly thank to Michał Praszalowicz for fruitful discussions and help during writing this work. I am very grateful to G.P. Korchemsky, A.N.Manashov and S.É. Derkachov whom I worked in an early state of this project. I also thank to Jacek Wosiek for illuminating discussions. This

work was supported by KBN PB 2-P03B-43-24, KBN PB 0349-P03-2004-27 and KBN PB P03B-024-27:2004-2007.

### References

- [1] M. Gell-Mann, M.L. Goldberger, F.E. Low, E. Marx, F.Zachariasen. Elementary particles of Conventional Field Theory as Regge poles. III. *Phys. Rev. B*, 133:145, 1964.
- [2] M. Gell-Mann, M.L. Goldberger, F.E. Low, E. Marx, F.Zachariasen. Elementary particles of Conventional Field Theory as Regge poles. IV. *Phys. Rev. B*, 133:161, 1964.
- [3] V. N. Gribov. A Reggeon diagram technique. *Sov. Phys. JETP*, 26:414–422, 1968.
- [4] V. S. Fadin, E. A. Kuraev, and L. N. Lipatov. On the Pommeranchuk singularity in asymptotically free theories. *Phys. Lett.*, B60:50–52, 1975.
- [5] J. Bartels. High-Energy behavior in a nonabelian gauge field theory. *Phys. Lett.*, B68:258, 1977.
- [6] H. Cheng and C. Y. Lo. High-energy amplitudes of Yang-Mills theory in arbitrary perturbative orders. 1. *Phys. Rev.*, D15:2959, 1977.
- [7] L. N. Lipatov I. I. Balitsky. The Pommeranchuk singularity in Quantum Chromodynamics. *Sov. J. Nucl. Phys.*, 28:822–829, 1978.
- [8] E. A. Kuraev, L. N. Lipatov, and V. S. Fadin. The Pommeranchuk singularity in nonabelian gauge theories. *Sov. Phys. JETP*, 45, 1977.
- [9] J. Bartels. High-energy behavior in a nonabelian gauge theory. 2. First corrections to  $T(n \rightarrow m)$  beyond the leading  $\ln s$  approximation. *Nucl. Phys.*, B175:365, 1980.
- [10] J. Kwiecinski and M. Praszalowicz. Three gluon integral equation and odd C singlet Regge singularities in QCD. *Phys. Lett.*, B94:413, 1980.
- [11] T. Jaroszewicz. High-energy multi - gluon exchange amplitudes. Triest preprint IC/80/175.
- [12] R. A. Janik and J. Wosiek. Solution of the odderon problem. *Phys. Rev. Lett.*, 82:1092–1095, 1999.
- [13] P. Gauron, B. Nicolescu, and L. Szymanowski. A possible field theoretical description of the odderon. IPNO/TH 87-53.
- [14] L. Lukaszuk and B. Nicolescu. A possible interpretation of p p rising total cross- sections. *Nuovo Cim. Lett.*, 8:405–413, 1973.
- [15] S. E. Derkachov, G. P. Korchemsky, and A. N. Manashov. Noncompact Heisenberg spin magnets from high-energy QCD. III: Quasiclassical approach. *Nucl. Phys.*, B661:533–576, 2003.
- [16] G. P. Korchemsky, J. Kotanski, and A. N. Manashov. Compound states of reggeized gluons in multi-colour QCD as ground states of noncompact Heisenberg magnet. *Phys. Rev. Lett.*, 88:122002, 2002.

- [17] S. E. Derkachov, G. P. Korchemsky, J. Kotanski, and A. N. Manashov. Noncompact Heisenberg spin magnets from high-energy QCD. II: Quantization conditions and energy spectrum. *Nucl. Phys.*, B645:237–297, 2002.
- [18] H. J. De Vega and L. N. Lipatov. Exact resolution of the Baxter equation for reggeized gluon interactions. *Phys. Rev.*, D66:074013, 2002.
- [19] H. J. De Vega and L. N. Lipatov. Interaction of reggeized gluons in the Baxter-Sklyanin representation. *Phys. Rev.*, D64:114019, 2001.
- [20] J. Kotanski. Three particle Pomeron and odderon states in QCD. 2005. hep-th/0603238.
- [21] Jan Kotanski. Reggeized gluon states in Quantum Chromodynamics. 2005. The PhD Thesis, hep-th/0511279.
- [22] M. A. Braun. *The interaction of reggeized gluons and Lipatov's hard pomeron*. – lectures. University of Santiago de Compostela, 17506 Santiago de Compostela, Spain, 1994.
- [23] G. 't Hooft. A planar diagram theory for strong interactions. *Nucl. Phys.*, B72:461, 1974.
- [24] L. N. Lipatov. Pomeron and odderon in QCD and a two-dimensional conformal field theory. *Phys. Lett.*, B251:284–287, 1990.
- [25] L. N. Lipatov. High-energy asymptotics of multicolor QCD and two-dimensional conformal field theories. *Phys. Lett.*, B309:394–396, 1993.
- [26] R. J. Baxter. *Exactly Solved Models in Statistical Mechanics*. Academic Press, London, 1982.
- [27] S. E. Derkachov, G. P. Korchemsky, and A. N. Manashov. Noncompact Heisenberg spin magnets from high-energy QCD. I: Baxter Q-operator and separation of variables. *Nucl. Phys.*, B617:375–440, 2001.
- [28] P. Di Francesco, P. Mathieu, D. Sénéchal. *Conformal Field Theory*. Springer, New York, 1982.
- [29] J. B. Zuber. An introduction to Conformal Field Theory. *Acta Phys. Polon.*, B26:1785–1813, 1995.
- [30] E. K. Sklyanin. Quantum inverse scattering method. Selected topics. 1991. hep-th/9211111.
- [31] L. D. Faddeev. Algebraic aspects of Bethe Ansatz. *Int. J. Mod. Phys.*, A10:1845–1878, 1995.
- [32] L. D. Faddeev. How Algebraic Bethe Ansatz works for integrable model. 1996. hep-th/9605187.
- [33] L. D. Faddeev, E. K. Sklyanin, and L. A. Takhtajan. The quantum inverse problem method. 1. *Theor. Math. Phys.*, 40:688–706, 1980.
- [34] J. Kotanski and M. Praszalowicz. Solutions of the quantization conditions for the odderon charge  $q_3$  and conformal weight  $h$ . *Acta Phys. Polon.*, B33:657–682, 2002.
- [35] G. P. Vacca. Properties of a family of  $n$  reggeized gluon states in multicolour QCD. *Phys. Lett.*, B489:337–344, 2000.



- [36] L. N. Lipatov. Duality symmetry of Reggeon interactions in multicolour QCD. *Nucl. Phys.*, B548:328–362, 1999.
- [37] J. Bartels, L. N. Lipatov, and G. P. Vacca. A new odderon solution in perturbative QCD. *Phys. Lett.*, B477:178–186, 2000.
- [38] G. P. Korchemsky. Bethe ansatz for QCD pomeron. *Nucl. Phys.*, B443:255–304, 1995.
- [39] T. Jaroszewicz. Infrared divergences and Regge behavior in QCD. *Acta Phys. Polon.*, B11:965, 1980.
- [40] L. A. Takhtajan and L. D. Faddeev. The quantum method of the inverse problem and the heisenberg xyz model. *Russ. Math. Surveys*, 34:11–68, 1979.
- [41] N. M. Bogolyubov, A. G. Izergin, and V. E. Korepin. *Quantum inverse scattering method and correlation functions*. Univ. Press, Cambridge, 1993.
- [42] L. N. Lipatov. High-energy asymptotics of multicolor qcd and exactly solvable lattice models. *JETP Lett.*, 59:596–599, 1994.
- [43] L. D. Faddeev and G. P. Korchemsky. High-energy QCD as a completely integrable model. *Phys. Lett.*, B342:311–322, 1995.